nks
Nordisk kernesikkerhedsforskning
Norrænar kjarnöryggisrannsóknir
Pohjoismainen ydinturvallisuustutkimus
Nordisk kjernesikkerhetsforskning
Nordisk kärnsäkerhetsforskning
Nordic nuclear safety research

NKS-160
ISBN 978-87-7893-225-9

Ex-Vessel Corium Coolability and Steam Explosion Energetics in Nordic Light Water Reactors

T.N. Dinh, W.M. Ma, A. Karbojian, P. Kudinov,
C.T. Tran and C.R. Hansson
Royal Institute of Technology (KTH), Sweden

March 2008

Abstract

This report presents advances and insights from the KTH's study on corium pool heat transfer in the BWR lower head; debris bed formation; steam explosion energetics; thermal hydraulics and coolability in bottom-fed and heterogeneous debris beds.

This report presents advances and insights from the KTH's study on corium pool heat transfer in the BWR lower head; debris bed formation; steam explosion energetics; thermal hydraulics and coolability in bottom-fed and heterogeneous debris beds.

Specifically, for analysis of heat transfer in a BWR lower plenum an advanced three-dimensional simulation tool was developed and validated, using a so-called effective convectivity approach and Fluent code platform. An assessment of corium retention and coolability in the reactor pressure vessel (RPV) lower plenum by means of water supplied through the Control Rod Guide Tube (CRGT) cooling system was performed. Simulant material melt experiments were performed in an intermediate temperature range (1300-1600K) on DEFOR test facility to study formation of debris beds in high and low subcooled water pools characteristic of in-vessel and ex-vessel conditions. Results of the DEFOR-E scoping experiments and related analyses strongly suggest that porous beds formed in ex-vessel from a fragmented high-temperature debris is far from homogeneous. Calculation results of bed thermal hydraulics and dryout heat flux with a two-dimensional thermal-hydraulic code give the first basis to evaluate the extent by which macro and micro inhomogeneity can enhance the bed coolability. The development and validation of a model for two-phase natural circulation through a heated porous medium and its application to the coolability analysis of bottom-fed beds enables quantification of the significant effect of dryout heat flux enhancement (by a factor of 80-160%) due to bottom coolant injection. For a qualitative and quantitative understanding of steam explosion, the SHARP system and its image processing methodology were used to characterize the dynamics of a hot liquid (melt) drop fragmentation and the volatile liquid (coolant) vaporization. The experimental results provide a basis to suggest that the melt drop preconditioning is instrumental to the subsequent coolant entrainment and resulting energetics of the so-triggered drop explosion. For steam explosion risk in reactors, a revisited study of the material property effect on steam explosion energetics showed that corium high density, high melting point and low conductivity are central to mechanisms in premixing that govern corium low explosivity.

Key words

Severe Accident, Corium, Debris Bed, Coolability, Steam Explosion

NKS-160
ISBN 978-87-7893-225-9

Electronic report, March 2008

The report can be obtained from
NKS Secretariat
NKS-776
P.O. Box 49
DK - 4000 Roskilde, Denmark

Phone +45 4677 4045
Fax +45 4677 4046
www.nks.org
e-mail nks@nks.org

Research Report

Ex-Vessel Corium Coolability and Steam Explosion Energetics in Nordic Light Water Reactors

T.N. Dinh, W.M. Ma, A. Karbojian, P. Kudinov
C.T. Tran and C.R. Hansson

Division of Nuclear Power Safety
Department of Physics, School of Engineering Sciences
Royal Institute of Technology (KTH)
106 91 Stockholm, Sweden

October 2007

Table of Contents

Executive Summary

Under the joint support of the 6th APRI (Accident Phenomena of Risk Importance), HSK, SARNET and NKS, the MSWI (Melt-Structure-Water-Interactions) project at the Royal Institute of Technology (KTH) has recently entered a new phase, which places the focus on assessment of ex-vessel melt risks in Nordic BWR plants with external cavity flooding. While combining both experimental and analytical studies, the present phase in the MSWI project pays an increased attention on scaling, simulation and support for plant safety analysis. Covering topics of importance to in-vessel corium coolability, steam explosion energetics and ex-vessel corium coolability, the work performed during 2006-2007 investigates selected MSWI phenomena which are identified as having the largest impact and significant uncertainties on the quantification of ex-vessel steam explosion and ex-vessel debris coolability. Substantial advances in process modeling and new insights into related mechanisms were gained from the study of corium pool heat transfer in the BWR lower head; debris bed formation; steam explosion energetics; thermal hydraulics and coolability in bottom-fed and heterogeneous debris beds.

Specifically, for analysis of heat transfer in a BWR lower plenum an advanced three-dimensional simulation tool was developed and validated, using a so-called effective convectivity approach and Fluent code platform. An assessment of corium retention and coolability in the reactor pressure vessel (RPV) lower plenum by means of water supplied through the Control Rod Guide Tube (CRGT) cooling system was performed. The analysis results reveal both the limit of coolability for CRGT and uncover possible vulnerabilities of the CRGT scheme for in-vessel melt retention. Simulant material melt experiments were performed in an intermediate temperature range (1300-1600K) on DEFOR test facility to study formation of debris beds in high and low subcooled water pools characteristic of in-vessel and ex-vessel conditions. Results of the DEFOR-E scoping experiments and related analyses strongly suggest that porous beds formed in ex-vessel from a fragmented high-temperature debris is far from homogeneous. Both high porosity and heterogeneity are central to the bed's enhanced dryout heat flux and therefore improved coolability. A comprehensive framework of phenomena feedbacks was introduced and advanced diagnostic and image processing techniques are examined to enable the next step in experimentation and quantitative analysis of complex multi-phase processes that govern debris bed formation. Calculation results of bed thermal hydraulics and dryout heat flux with a two-dimensional thermal-hydraulic code give the first basis to evaluate the extent by which macro and micro inhomogeneity can enhance the bed coolability. The development and validation of a model for two-phase natural circulation through a heated porous medium and its application to the coolability analysis of bottom-fed beds enables quantification of the significant effect of dryout heat flux enhancement (by a factor of 80-160%) due to bottom coolant injection. For a qualitative and quantitative understanding of steam explosion, a new system (named SHARP) was developed to synchronize high-speed digital cinematography and x-ray radiography for multi-fluid multiphase visualization. The SHARP and its image processing methodology was used to characterize the dynamics of a hot liquid (melt) drop fragmentation and the volatile liquid (coolant) vaporization. The experimental results provide a basis to suggest a so-called melt drop preconditioning i.e. deformation/pre-fragmentation of a hot melt drop immediately following the pressure trigger, being instrumental to the subsequent coolant entrainment and resulting energetics of the so-triggered drop explosion. For steam explosion risk in reactors, a revisited study of the material property effect on steam explosion energetics showed that corium high density, high melting point and low

conductivity are central to mechanisms in premixing that govern corium low explosivity. A new hypothesis was provided for rationalizing the effect of the corium composition (eutectic *vs*. non-eutectic) on its triggerability and energetics.

Overall, the MSWI research in 2006-2007 has advanced the knowledge of Melt-Structure-Water Interactions toward reducing conservatism in quantification of ex-vessel melt risks in Nordic BWRs.

Due to space constraint, this report just summarized the key points of the project progress and achievements. Detailed technical description and more items of the progress can be found in the References listed at the end of the report.

Acknowledgement

The support for the MSWI Project by the APRI Consortium (Forsmark, Oskarshamn, Ringhals, SKI), the European Commission (SARNET NoE), the Nordic Nuclear Safety Programme (NKS), the Swiss Nuclear Safety Committee HSK is gratefully acknowledged. The authors thank Prof. B.R. Sehgal (KTH), Prof. W. Frid (SKI), Dr. N. Garis (SKI), Dr. O. Sånderväg (SKI), Mr. L. Agrenius (APRI), Mr. P. Isaksson (Vattenfall, NKS), Mr. V. Gustaffson (Vattenfall), Mr. A. Henoch (Ringhals), and Dr. R. Schulz (HSK) for their insights, constructive criticism, continued interest and support for this project over the years. The dedicated and professional support from NPS Laboratory staff Mr J. Galdo, Mr. G. Adlin in experiments, and Mr S. Roshan in computer infrastructure is also acknowledged.

1. Introduction

1.1. Project goals

The central aim of the MSWI (Melt-Structure-Water Interactions) project at Royal Institute of Technology (KTH) is to create new knowledge on melt-structure-water-interaction phenomena (e.g. data, insights, models, codes and methodology) which enables reducing uncertainty in quantification of severe accident risks in a light water reactor (LWR). Supported by the APRI group (including SKI and Swedish utility), HSK, Nordic Nuclear Safety Program (NKS) and European Union (SARNET project), the MSWI research's driving force and immediate objectives are to build a sound foundation that helps bring to the resolution two long-standing severe accident issues in nuclear power plants, namely steam explosion and corium (debris) coolability in in-vessel and ex-vessel scenarios of severe accidents. Overall project objectives are shown on Figure 1.

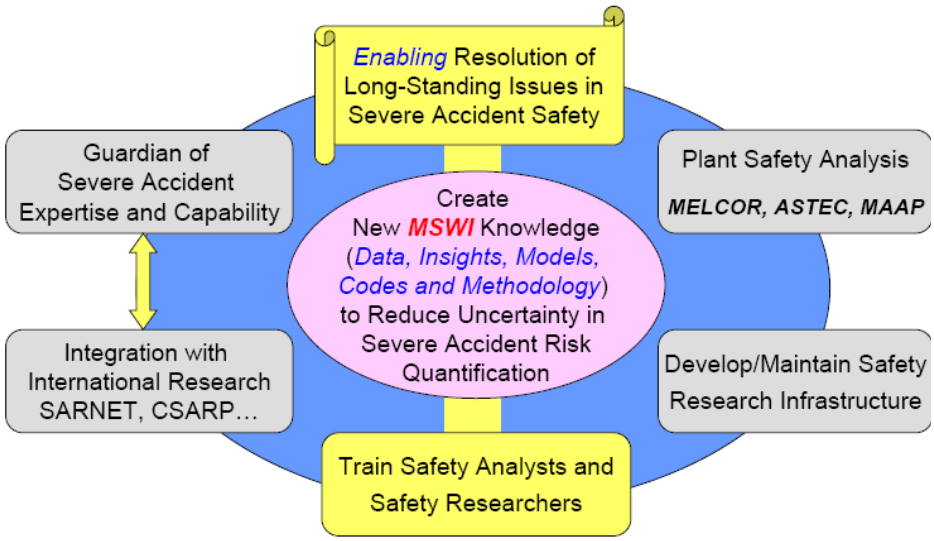

Figure 1: MSWI Project Objectives.

More specifically, topical areas covered during 2006-2008 period include in-vessel debris coolability and retention (INCO), ex-vessel debris coolability (EXCO), and steam explosion energetics (SEE). The present report focuses on work and results carried out in INCO and EXCO topics, with the objectives to:

- Develop and validate a suitable tool for effective simulation of heat transfer in a core melt pool formed in the complex geometry of a BWR lower plenum;
- Study the effectiveness and vulnerability of in-vessel corium melt pool coolability by coolant flow in control rod guide tubes (CRGTs)
- Perform exploratory test for DEFOR (debris bed formation) program;
- Provide a scoping analysis and scaling rationale for DEFOR snapshot test program;
- Examine the effect of the coolant bottom-fed on debris coolability
- Apply an advanced analysis method to evaluate the potential effect of debris bed inhomogeneity on its coolability.
- Visualize micro interactions of steam explosion and qualify its mechanisms.
- Address the effects of corium physical properties and compositions on steam explosion.

1.2. Project approach

Since the MSWI research is directed toward addressing ex-vessel melt risks, a risk-oriented approach is used to guide the analytical and experimental activity. Our emphasis is to identify and study phenomena which have potential to serve as limiting mechanism for threats which challenge the containment integrity. We emphasize the significance of relating phenomena and processes which have previously been taken for separate investigations (in a divide-and-conquer strategy). Special attention is paid on scaling, simulation and support for plant safety analysis.

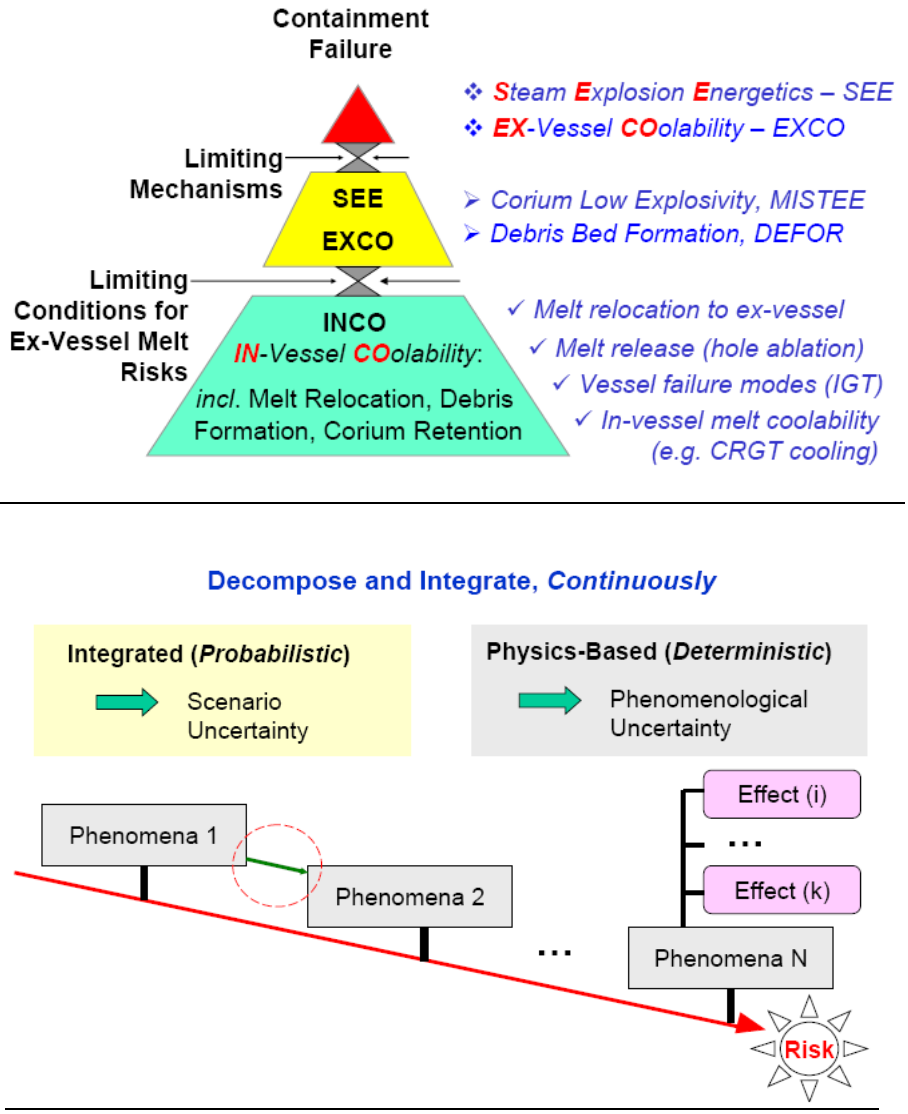

Figure 2: Risk-Oriented Approach is used for activity integration and synergy.

1.3. Work and results in brief

In what follows we provide a short synopsis of works carried out and results obtained in 8 tasks. Detailed description is provided in subsequent sections for each corresponding Part.

***Part A*: An Effective Convectivity Model for Simulation of In-Vessel Core Melt Progression in Boiling Water Reactor**

This part is concerned with development and application of a so-called Effective Convectivity Model (ECM), which aims to provide a detailed, mechanistic description of heat transfer processes in a BWR lower plenum. The ECM is a Computational Fluid Dynamics (CFD)-like tool which employs a simpler and more effective approach to compute heat transfer by solving only energy conservation equation instead of solving the full set of Navier-Stokes and energy equations by a CFD code. We implement the ECM on a CFD code (Fluent), detailed description of the ECM development, implementation and validation is given. A dual approach is used to validate the ECM, namely validation against experimental data and heat transfer results obtained by CFD predictions in the same geometries and conditions. Insights gained from CFD simulations are also used to improve ECM. The ECM capability as an effective tool to simulate heat transfer of an internally heated volume in 3D complex geometry is demonstrated through examples of heat transfer analysis in a BWR lower plenum being cooled by coolant flow in Control Rod Guide Tubes. Simulation results and key findings of this case are reported and discussed.

***Part B:* Analysis of melt pool coolability in a BWR lower head by coolant flow in CRGTs**

This part is concerned with progression of a severe core melt accident in a BWR. Of interest here is assessment of corium retention and coolability in the reactor pressure vessel (RPV) lower plenum by means of water supplied through the Control Rod Guide Tube (CRGT) cooling system. The question arose on whether the CRGT cooling as a mitigation measure is sufficient to prevent the RPV failure with subsequent melt discharge. The analysis performed reveals both the limit of coolability for CRGT and uncover possible vulnerabilities of the CRGT scheme for in-vessel melt retention.

***Part C:* A scoping study of debris formation in DEFOR experimental facility**

In this part, we discuss results obtained in a scoping series of a new experimental program at the Division of Nuclear Power Safety (NPS) Royal Institute of Technology (KTH). The experimental program was initiated to study the processes which govern debris bed formation (DEFOR) during severe accident with core melt down and reactor pressure vessel failure at LWR plant. The objective of the present exploratory phase (DEFOR-E) is to test operational concepts, and initiate the analysis of DEFOR related phenomena. Binary oxides mixtures at different overheating were used as corium melt simulants. Sensitivity of debris bed properties to water pool depth and subcooling is discussed in the part. The insights gained from the scoping experiments are found useful to guide the scaling rationale and design of the next series of “Snap-Shot” experiments in DEFOR.

Part D: **A study on ex-vessel debris formation in a LWR severe accident**

In this part we analyze phenomena that govern debris formation and introduce a comprehensive framework to exhibit their interrelationship during a hypothetical severe accident in a BWR. We focus on phenomena feedbacks and identify key parameters which are believed to have significant effect on debris packing, including boiling regimes on fragments, their settling against steam flow stemming from a bottom bed. Based on scoping calculations for reactor scenarios, the prototypic range of the key parameters is delineated. Taking into account the practical and technical constraints of laboratory experiments with simulant fluids and results from calculations for experimental conditions, we establish feasibility and parameter ranges under which new DEFOR-S "snap-shot" experiments shall be conducted to provide reactor relevant data and insights. Requirements on experimental measurements are also discussed in the study.

Part E: **Coolability of a bottom-bed debris bed**

This work investigates the potential effectiveness of natural circulation-driven coolability (NCDC) as a severe accident mitigative measure. The NCDC can particularly be useful in LWR plants which employ external cavity flooding. The main idea is to provide a simple design solution that facilitates bottom feeding of coolant into the debris bed, and uses steam production in the decay-heated debris bed to drive the two-phase flow natural circulation. We use an analytical one-dimensional model to calculate characteristics of two-phase thermal-hydraulics in porous media. The model employs Lockhart-Martinelli correlations for two-phase flow friction and void fraction, and Ergun's correlation for single-phase flow resistance. Adaptation and verification of the model are discussed in this part. Coolability of debris beds with coolant bottom-fed is evaluated for a broad range of conditions. The analysis suggests that the dryout heat flux (DHF) in bottom-fed configurations can be increased by 80% to 160%, when compared to DHF in top-flooding beds.

Part F: **Analysis of the effect of debris bed inhomogeneity on its coolability**

The present study investigates the potential impact of bed inhomogeneity on coolability of volumetrically heated debris beds which may form in a hypothetical severe accident in a LWR. Specifically, we examine the effect of the debris bed's micro and macro heterogeneity (in term of particle size and pore distributions in space). A vehicle for the analysis is WABE-2D code which simulates two-phase thermal-hydraulics in porous bed. The present analysis is performed for two types of "unit volume" which correspondingly represent the macro-heterogeneous bed and micro-heterogeneous bed. Results of calculation of dryout heat flux with WABE-2D code show the extent by which macro and micro inhomogeneity can enhance the bed coolability. Phenomenologically, in both cases, inhomogeneity is found to facilitate natural circulation driven coolability (NCDC) which helps overcome the counter-current flow limitation. Implications of the findings on assessment of debris bed coolability and related research are discussed in this part.

Part G: **Dynamics and preconditioning in a single drop vapor explosion**

To pursue a qualitative and quantitative understanding on the vapor explosion phenomena, the SHARP (**S**imultaneous **H**igh-speed **A**cquisition of x-ray **R**adiography and **P**hotography) system, was developed to visualize both material dynamics and interface dynamics of multi-fluid multiphase flow. The SHARP system and its image processing enable new insights into the physics of the vapor (steam) explosion phenomena as well as quantitative information of the associated dynamic micro-interactions. For instance, analysis of the experimental results shows that, following an external perturbation (trigger), a high temperature molten material (tin) drop underwent deformation and partial fragmentation already during the first cycle of bubble growth. Further analysis of the SHARP data reveals the relation between the drop's dynamics in the first bubble cycle and the energetics of the subsequent explosive evaporation in the second cycle. This finding provides a basis to suggest a so-called melt drop preconditioning i.e. deformation/ pre-fragmentation of a hot melt drop immediately following the pressure trigger, being instrumental to the subsequent coolant entrainment and resulting energetics of the so-triggered drop explosion.

Part H: **Material property effect in steam explosion energetics: *Revisited***

Steam explosion, as a threat to LWR reactor vessel and containment integrity, has been postulated to occur during a hypothetical severe accident with relocation of molten core materials to a water pool either in-vessel or ex-vessel. Studies of molten fuel-coolant interactions (FCI) conducted over the past decades have not resolved the controversy about whether, when, and how melt material properties influence steam explosion energetics. Crucial questions persist about safety significance of experimental evidence about corium low explosivity in various reactor accident scenarios. In this study, taking into consideration results from recent FCI experiments and analyses, we revisit the study of Dinh et al (1998) and hypotheses proposed therein about mechanisms by which corium physical properties may influence steam explosions. Corium high density, high melting point and low conductivity are found to be central to mechanisms in premixing that govern corium low explosivity. For micro-interactions, three processes, namely drop surface undercooling, nucleation and growth of solid phases, and interfacial instability and breakup are evaluated with respect to their role in fine fragmentation. The current study provides a new hypothesis for rationalizing the effect of corium composition (eutectic vs. non-eutectic) on its triggerability and energetics.

2. Work and Results in Detail

2.1. *Part A:* An effective convectivity model for simulation of in-vessel core melt progression in a boiling water reactor

2.1.1. Introduction

This study is concerned with the development and application of an effective tool capable of simulating heat transfer of a melt pool in a BWR lower plenum.

CFD methods have been extensively used to analyze turbulent natural convection heat transfer in volumetrically heated liquid pools, representative of corium pools in a Reactor Pressure Vessel (RPV) lower plenum during a severe core-melting accident. Such CFD simulations, although limited to simple pool geometries and lower range of Rayleigh number, were conducive to basic understanding of complex fluid physics in reactor accident situations. However, for long-term transients in reactor-scale situations with highly-developed surface areas such as in a BWR lower plenum, CFD simulations remain prohibitively expensive. Analytical models based on experimental correlations were also devised and used to calculate heat transfer of a melt pool. However the questions remain on which correlations should be used for heat transfer on the CRGT cooled walls and the vessel wall, and how to apply them in the real geometry of a melt pool with a forest of cooled penetrations (CRGTs) and uncooled ones, such as Instrumentation Guide Tubes (IGTs).

In this study, we introduce a new model called Effective Convectivity Model (ECM), which will be implemented in a CFD code to simulate heat transfer of a core melt pool in a BWR lower plenum. Validation of ECM is performed by dual approach: the first approach is to compare the results of ECM heat transfer with existing experimental data, and the second approach is to compare the predicted results of the ECM with those of CFD simulation under the same geometry and conditions.

2.1.2. Technical approach

Built on the concept of effective convectivity first introduced in ECCM [3, 4], the ECM method uses a characteristic velocities U_x, U_y and U_z to effectively transfer the heat generated in a fluid volume toward the cooled wall in an amount equal to the convective heat transport in the respective direction. The characteristic velocities are determined by means of heat transfer correlations.

The use of effective convectivity helps eliminate the need to solve a complete set of Navier-Stokes and energy equations with fluid velocities (u_x, u_y and u_z) – a computationally expensive exercise for a large pool with high Rayleigh numbers (turbulent natural convection). Instead, the following energy conservation equation with effective convective terms (with characteristic velocities U_x, U_y and U_z) is solved:

$$\frac{\partial\left(\rho C_p T\right)}{\partial t}+\left(\frac{\partial\left(\rho C_p U_x T\right)}{\partial x}+\frac{\partial\left(\rho C_p U_y T\right)}{\partial y}+\frac{\partial\left(\rho C_p U_z T\right)}{\partial z}\right)=k.\nabla^2 T+Q_v \qquad \text{(A-1)}$$

Equation (A-1) is essentially a heat conduction equation once the effective convective terms are moved to the right hand side, serving as a source term.

To take advantages of a commercial CFD code in calculating heat transfer of a melt pool in a complex geometry, the ECM is implemented in the Fluent code using its User Define Function (UDF) [6]. The source term in the conduction equation solved in Fluent is modified as:

$$Q_v - \left(\frac{\partial(\rho C_p U_x T)}{\partial x} + \frac{\partial(\rho C_p U_y T)}{\partial y} + \frac{\partial(\rho C_p U_z T)}{\partial z} \right) \quad \text{(A-2)}$$

In reality, the effective convective heat transport term is active only at the pool boundaries. To achieve the pool's correct energy balance, the convective heat transport term added in the pool is uniformly removed from the whole computational domain. The procedure is detailed in [2].

The implementation of ECM in Fluent offers advantages of being able to use the Fluent/Gambit/TGrid grid generator to create 3D grid, and consequently perform simulation in a 3D geometry and post processing of the corresponding results. Later, the ECM is used in conjunction with a phase-change model in Fluent to compute the pool formation process.

2.1.3. Validation

Experimental data used for validation of the ECM include (i) transient temperature profiles of Kulacki & Emara's experiment with fluid layer cooled from the top [7]; (ii) Kulacki & Goldstein experiment with fluid layers cooled from the top and bottom [8]; and (iii) Steinberner & Reneike experiment with volumetrically heated water in square cavity cooled from the top, bottom and vertical walls [5].

Kulacki et al. reported measurements of transient temperature distribution of an internally heated horizontal fluid layer cooled from the top [7]. The ECM simulation results of transient temperature profiles (*lines*) are in a good agreement with the experimental data (Figure A-1).

Kulacki & Goldstein recorded temperature profiles of internally heated fluid layers cooled from the top and bottom with wide range of Rayleigh numbers [8]. The ECM simulation of the experiments showed comparable temperature profiles with the experimental data (Figure A-2).

A simple analytical model based on energy balance and experimental correlations is used to calculate energy splitting (heat fluxes) in Steinberner and Reneike experiments with internally heated water in a square cavity cooled from the top, bottom and vertical walls [5]. Results of CFD prediction, ECM simulation and the analytical model (using Steinberner & Reneike's correlations) are as shown in Table A-1 to demonstrate a reasonably good agreement (within 15%). As expected, the ECM simulation (also using Steinberner-Reineke correlations) produces better agreement with the analytical model than the CFD simulation.

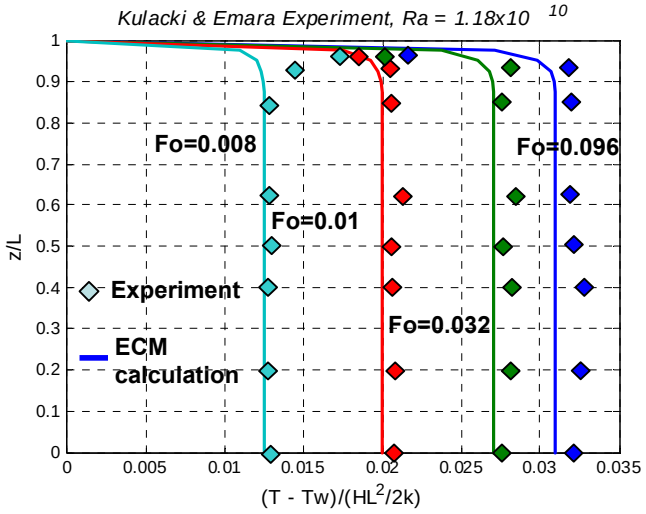

Figure A-1: Transient temperature profiles ($Ra=1.18x10^{10}$) in a fluid layer cooled from the top

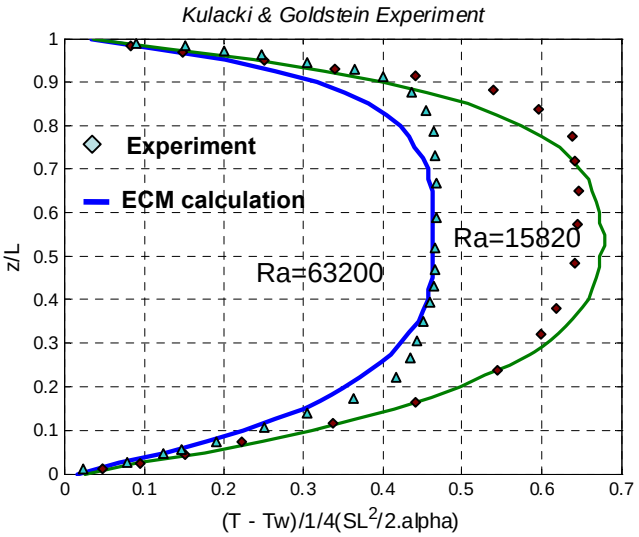

Figure A-2: Temperature profiles in fluid layers cooled from the top and bottom

Further validation of the ECM is made by comparison with CFD simulation of heat transfer in a melt pool in a scaled PWR lower plenum. Results of simulations by CFD and ECM methods can be found in our paper [2], which shows that a fairly good agreement was achieved. Notably, the difference of the maximum temperature predicted by the two methods is 11K.

Table A-1: CFD, ECM simulations and analytical model results

Models	q_{up}, W/m^2	q_{side}, W/m^2	q_{down}, W/m^2
CFD	1045	599	41
ECM	953	696	48
Analytical	1026	659	55

As an example of heat transfer simulation for a 3D complex geometry, we apply the ECM method to a melt pool unit volume in a BWR, for which CFD simulation was also performed and presented in [1]. Specifically, a unit volume is a rectangular box surrounding one CRGT and filled with the decay-heated corium. The results show that the maximum temperatures of the core melt obtained by two methods differ by mere 5K.

Thus, the ECM predictions are in a good agreement with both experimental data and results of CFD simulations. The simulations for the unit volume show the difference in heat fluxes predicted by CFD and ECM is acceptable (within 15% for upward and sideward heat fluxes).

2.1.4. Heat transfer of a core melt pool in a BWR lower plenum

Finally, the ECM is applied to simulate heat transfer of a corium pool formed in a BWR lower plenum. The BWR lower plenum compared to that of a PWR includes a large number of CRGTs and IGTs. It was proposed that the coolant flow in CRGTs be used to enhance coolability of debris and core melt pool formed in the lower plenum. The lower plenum, CRGT number and arrangement vary in different designs. In the present study we use an ABB-ATOM reactor configuration which contains 121 CRGTs. Configuration of a part of the lower plenum under consideration can be seen in Figure A-3.

The ECM is used to simulate a 3D slice of a melt pool with 6 CRGTs inside (Figure A-3). Boundary conditions applied in the ECM simulation are: the front surface is symmetrical; the back surface is adiabatic; the CRGT walls, top and vessel walls are isothermal; the left wall of the slice can be set symmetrical as well as adiabatic boundary condition. Results of the ECM simulation of a melt pool with height of 1.4m are presented in Figure A-4.

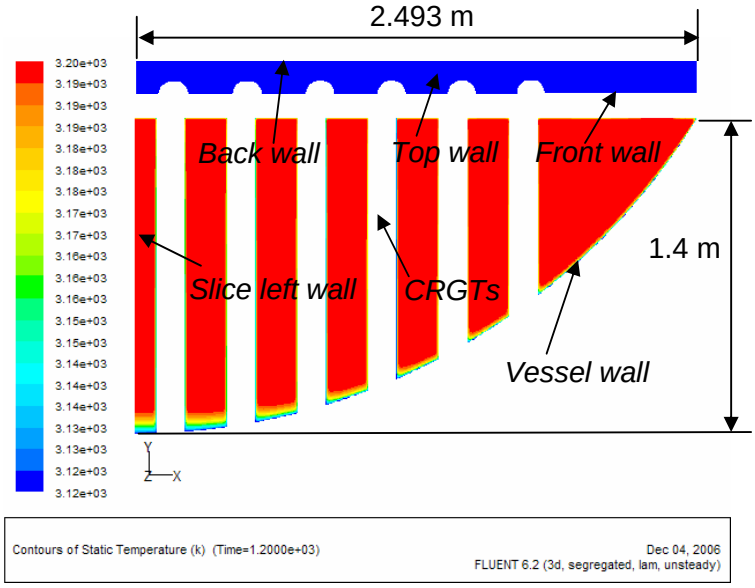

Figure A-3: Temperature field in a lower plenum slice.

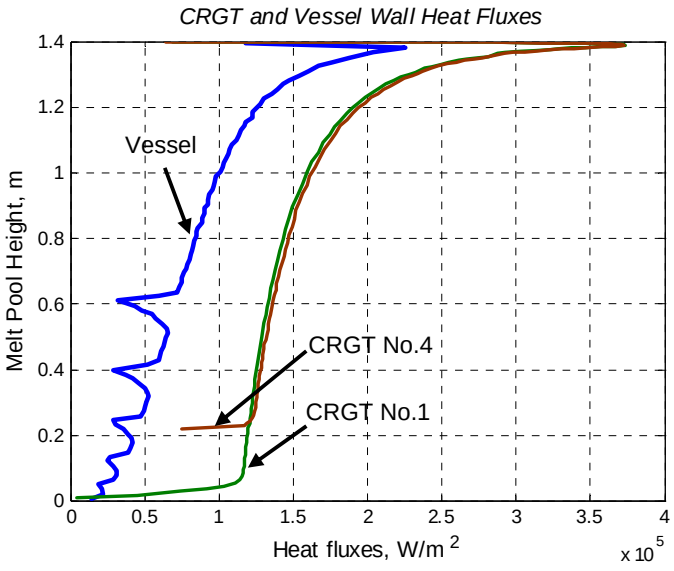

Figure A-4: CRGT and vessel wall heat fluxes.

It can be seen from the simulation results that heat flux distributions along the CRGTs are very close in both profile and value. The maximum value of CRGT heat flux profile is found to be close to 400kW/m^2 for the pool with height of 1.4m. Superheat of the core melt is less than 100K. The CRGT wall heat flux is higher than the vessel wall heat flux (Figure A-4). The peaking value of CRGT wall heat flux is 1.7 times higher than the peaking value of the vessel wall. Further analysis is needed to identify weaker regions in a CRGT and vessel walls. CRGT walls are vulnerable due to high heat fluxes and smaller wall thicknesses, while the lower plenum vessel wall is amenable to ablation due to absence of external surface cooling in BWRs.

2.1.5. Concluding remarks

The present work is built on the original concept of Effective Conductivity-Convectivity Model (ECCM) first proposed in 1996 by Bui and Dinh [3]. The ECCM is revised in the present work, and the new Effective Convectivity Model (ECM) is implemented in a commercial CFD code Fluent to enable simulation of heat transfer of a melt pool in a BWR lower plenum.

We demonstrate that the ECM is capable of predicting maximum temperature range and heat fluxes of an enveloped, 3D, large-size and complex-geometry melt pool such as in a BWR lower head with penetration forest.

The ECM is not only limited to simulation of enveloped scenarios, but also can be extended to simulation of stratified melt pools and evolving melt pools due to phase changes such as in scenarios with core melt pool formation. These extensions and applications are underway and documented in another paper.

References of Part A

[1] C. T. Tran, T. N. Dinh, "Analysis of melt pool heat transfer in a BWR lower head", Transaction, *ANS Winter Meeting*, Albuquerque, NM, USA, November 12-16, 2006.

[2] C.T. Tran and T.N. Dinh, "An effective convectivity conductivity model for simulation of in-vessel core melt progression in boiling water reactor", The 2007 International Congress on Advanced Nuclear Power Plants, Nice, France. May 13-18, 2007.

[3] V. A. Bui and T. N. Dinh, "Modeling of heat transfer in heated-generating liquid pools by an effective diffusivity-convectivity approach", *Proceedings of 2nd European Thermal-Sciences Conference*, Rome, Italy, pp.1365-1372, 1996.

[4] B. R. Sehgal, V. A. Bui, T. N. Dinh and R. R. Nourgaliev, "Heat transfer process in reactor vessel lower plenum during a late phase of in-vessel core melt progression", *J. Advances in Nuclear Science and Technology*, Plenum Publ. Corp., 1998.

[5] U. Steinberner and H.H. Reineke, "Turbulent buoyancy convection heat transfer with internal heat sources", *Proceedings of the 6th Int. Heat Transfer Conference*, Toronto, Canada, Vol.2, pp.305-310 (1978).

[6] UDF Manual, *FLUENT 6.2 Documentation*, Fluent Inc. 2005.

[7] F. A. Kulacki and A. A. Emara, "Steady and transient thermal convection in a fluid layer with uniform volumetric energy sources", *J. Fluid Mech.*, Volume 83, part 2, pp.375-395, 1977.

[8] F.A. Kulacki and R.J. Goldstein, "Thermal convection in a horizontal fluid layer with uniform volumetric energy sources", *J. Fluid Mech*. Volume 55, part 2, 271-287 (1972).

2.2. *Part B:* Analysis of melt pool coolability in a BWR lower head by coolant flow in control rod guide tubes (CRGTs)

2.2.1. Introduction

The present study is concerned with progression of a severe core melt accident in a BWR. Of interest here is assessment of corium retention and coolability in the reactor pressure vessel (RPV) lower plenum by means of water supplied through the Control Rod Guide Tube (CRGT) cooling system [1]. The question arose on whether the CRGT cooling as a mitigation measure is sufficient to prevent the RPV failure with subsequent melt discharge.

2.2.2. Description of work

The initial objective is to compute and relate thermal loading on the CRGT to critical heat flux (CHF) in them, while assuming the reactor's drain lines and instrument guide tubes being plugged to inhibit core melt discharge. An analytical energy-balance model is applied and complemented with a Computational Fluid Dynamics (CFD) study. In both cases, a unit cell (rectangular box surrounding one CRGT and filled with the decay-heating corium) is considered. In a thermally enveloping scenario of in-vessel melt retention the unit contains a quasi-steady-state corium pool isothermally cooled on all boundaries. The analytical treatment uses heat transfer correlations ($Nu_{up} = 0.345.Ra^{0.233}$; $Nu_{sd} = 0.85.Ra^{0.19}$; $Nu_{down} = 1.389.Ra^{0.095}$) obtained previously by Steinberner and Reineke in experiments for volumetrically-heated liquid pools [2]. The validity of these correlations was confirmed in other experiments [3] [4].

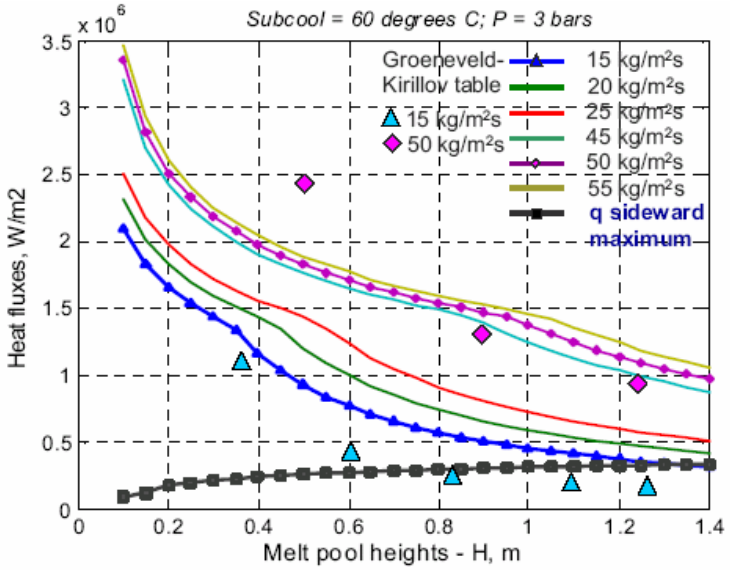

Figure B-1: Thermal loading on the CRGT (shown as q_sideward maximum) and CHF. The dots are based on a CHF lookup table [8]; the curves are calculated by a model [9] for different coolant flow rate.

The CFD study employs Fluent code to compute turbulent natural convection flow and heat transfer in the unit cell. A fine nodalization was applied to effectively provide large-eddy simulation without an explicit subgrid scale model [5] [6]. Extensive validation over a relevant range of Rayleigh numbers (10^{11}-10^{15}) was performed [7].

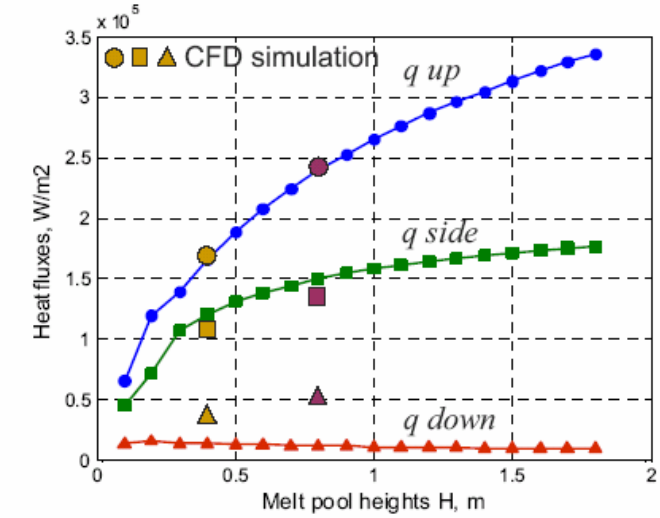

Figure B-2: Thermal loadings in a unit cell: CFD vs. analytical model.

2.2.3. Results

At the operational flow rate of 15 kg/(m^2.s), thermal loadings from the melt pool imposed on the CRGT wall are predicted to be below the CHF for corium pool height up to 0.7m. However, for such low flow rates, uncertainty in CHF prediction is found to be significant. Increase of flow rate to 30 kg/(m^2.s) and higher in CRGTs increases the coolability range (Figure B-1). As the pool height increased above 1m, the fraction of heat removed through the CRGT reaches 75-80%.

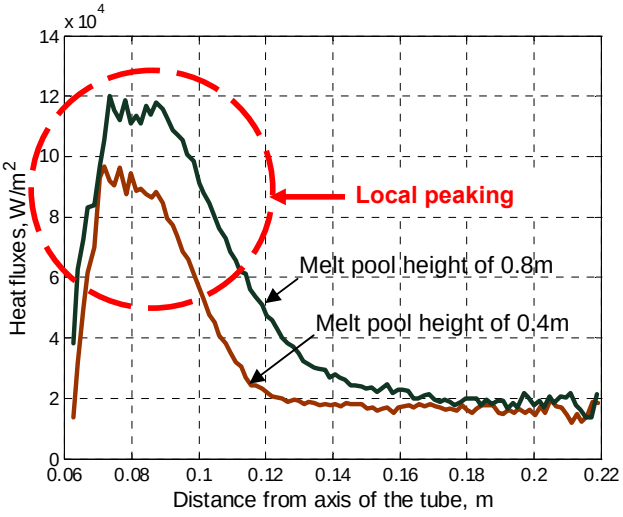

Figure B-3: Downward heat flux distribution across the CRGT unit cell.

The upward and sideward heat fluxes computed by CFD and analytical model agree well, whereas the surface-averaged downward heat fluxes substantially differ (Figure B-2). Analysis of the computed results revealed a locally enhanced flux near the cooled CRGT wall (Figure B-3). This is consistent with the impingement of descending flow related to "low Prandtl number effect", previously reported for corium pools in [10]. Without external cooling, high downward heat fluxes from the corium pool would cause a rapid ablation of the RPV wall. Most importantly, the impingement of flow descending along the vertical CRGT cooled wall is likely to cause local vessel melt-through leading to melt discharge as a film along the ex-vessel part of the control rod driver. Despite of the high cooling capacity of CRGTs and their potential role in delaying the vessel failure, the present study identified downward heat fluxes as the primary threat to the BWR vessel integrity in thermally enveloping scenarios of in-vessel coolability. An external vessel cooling would significantly increase the likelihood of in-vessel retention.

References of Part B

[1] A. Jasiulevicius, B.R. Sehgal, "COMECO experiments on molten pool coolability enhancement in the BWR lower head with CRGTS", *The 10th International Meeting on Nuclear Reactor Thermal Hydraulic (NURETH-10)*, Seoul, Korea, October 5-9, 2003.

[2] U. Steinberner and H.H. Reineke, "Turbulent buoyancy convection heat transfer with internal heat sources", *Proceedings of the 6th Int. Heat Transfer Conference*, Toronto, Canada, Vol.2, pp.305-310 (1978).

[3] T.G. Theofanous, S. Angelini, "Natural convection for in-vessel retention at prototypic Rayleigh number", *Journal of Nuclear Engineering and Design*, v. 200, pp 1-9 (2000).

[4] T.G. Theofanous, C. Liu, S. Additon, S. Angelini, O. Kymalainen and T. Salmassi, "In-vessel coolability and retention of a core melt", *DOE/ID-1046*, November 1994.

[5] R.R. Nourgaliev and T.N. Dinh, "An investigation of turbulence characteristics in an internally heated unstably stratified fluid layer", *Journal of Nuclear Engineering and Design*, v.178, pp.235-258 (1997).

[6] T.N. Dinh, Y.Z. Yang, J.P. Tu, R.R. Nourgaliev and T.G. Theofanous, "Rayleigh-Benard natural convection heat transfer: pattern formation, complexity and predictability", *Proceedings of ICAPP ´04*, Pittsburgh, PA USA, June 13-17, paper 4241 (2004).

[7] F.A. Kulacki and R.J. Goldstein, "Thermal convection in a horizontal fluid layer with uniform volumetric energy sources", *J. Fluid Mech*. Vol.55, part 2, 271-287 (1972).

[8] D.C. Groeneveld, L. K. H. Leung, P.L. Kirillov, V.P. Bobkov, I.P. Smogaliev, V.N. Vinogradov, X.C. Huang, E. Royer, "The 1995 look-up table for critical heat flux in tubes", *Journal of Nuclear Engineering and Design*, V.163, pp. 1-23 (1996).

[9] Y. Katto, "General features of chf of forced convection boiling in vertical concentric annuli with a uniformly heated rod and zero inlet subcooling", *Journal of Heat Mass Transfer*, Vol.2, pp. 109-116 (1981).

[10] R. R. Nourgaliev, T.N. Dinh and B.R. Sehgal, "Effect of fluid prandtl number on heat transfer characteristics in internally heated liquid pools with Rayleigh numbers up to 10^{12}", *Journal of Nuclear Engineering and Design*, V.169, pp.165-184 (1997).

2.3. *Part C:* A scoping study of debris formation in DEFOR experimental facility

2.3.1. Introduction

The objectives of DEFOR program are addressed in Part D, and not repeated here. It is hoped that studies of DEFOR experiments on melt fragmentation and debris bed formation may provide observations and data to develop a better understanding and tools for prediction of the phenomena. The present study is related to DEFOR-E scoping experiments, whose focus is placed on the test facility commissioning and preliminary study on the influence of *(i)* water subcooling and pool depth, *(ii)* melt material composition and superheat, and *(iii))* two-phase thermo-hydraulics on the debris bed properties (porosity, particle size distribution and morphology) which are related to coolability. More detailed results can be found in [4].

2.3.2. Experimental facility and procedure

The main aim of DEFOR experimental facility is to provide platform of experiments with various simulant materials under different conditions and with variation of governing parameters in wide ranges. The facility design also enables the visualization and measurements of the transient experimental processes.

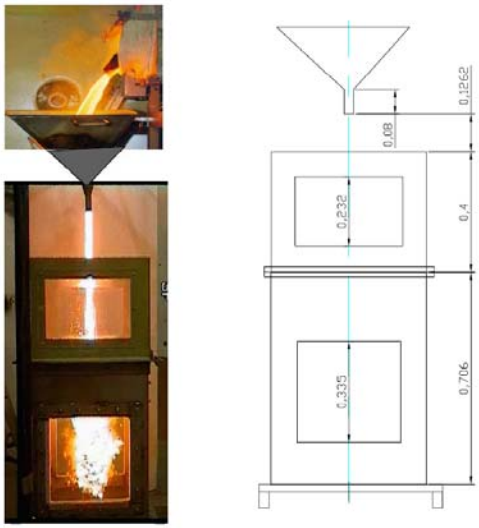

Figure C-1: DEFOR facility dimensions and illustration.

A schematic view of DEFOR experimental facility is shown in Figure C-1, mainly composed of the upper section with melt Induction-Furnace (IF), melt delivery funnel, and the lower section with glass/steel walled coolant tank. The melt is generated inside a cylindrical silicon carbide crucible with volume/capacity of 15 liters heated by an induction furnace of medium frequency up to 30 kHz and max power of 45 kW. The liquid melt is delivered to the funnel by tilting the crucible remotely. The delivery funnel consists of an accumulator with a nozzle at the bottom. The jet formed at the nozzle outlet is gravity driven and melt release duration depends on melt volume used and the chosen nozzle outlet diameter. Thermocouples are used to measure the temperature of the

melt and debris bed, and video cameras are employed for visual observation of the jet fragmentation process.

Table C-1 lists 7 experiments performed in DEFOR-E scoping experiments. In the first 6 experiments a binary oxide of glass type mixture CaO-B_2O_3 was used. The last experiment (exp-7) was performed using a more heavy oxide mixture of ceramic type material WO_3-CaO.

Table C-1: DEFOR experimental conditions and main results.

№	Parameter/Property	exp-1	exp-2	exp-3	exp-4	exp-5	exp-6	exp-7
1	Melt volume, liters	3.5	7.0	3.5	3.5	3.5	3,5	2,5
2	Melt initial temperature, ^oC	1200	1300	1350	1350	1200	1250	1280
3	Coolant volume, liters	163	163	163	100	100	163	163
4	Coolant initial temperature, ^oC	13	11	85	15	83	88	7
5	Water pool depth, cm	65	65	65	40	40	65	65
6	Falling height, cm	60	60	60	60	60	60	60
7	Measured porosity, %	60	77	74	56	50	68	65

2.3.3. Experimental results

Figure C-2 shows the photo sequence of the melt pouring and fragmentation process. The results obtained from the experiments showed that the size distribution and morphology of the solidified debris are strongly determined by the coolant temperature. In highly subcooled tests, DEFOR-01, DEFOR-02, DEFOR-04 and DEFOR-07 the jet breaks up into a large number of totally fragmented irregular particles with different sizes and shapes. The debris at the bottom of the water tank forms a heap-like shape bed (Figure C-3).

The post-test analysis showed that the bed was stratified and was inhomogeneous. The measured averaged porosities in DEFOR-01, DEFOR-02, DEFOR-04 and DEFOR-07 experiments were round 60%, which is similar to that obtained in CCM and FARO tests [1-3]

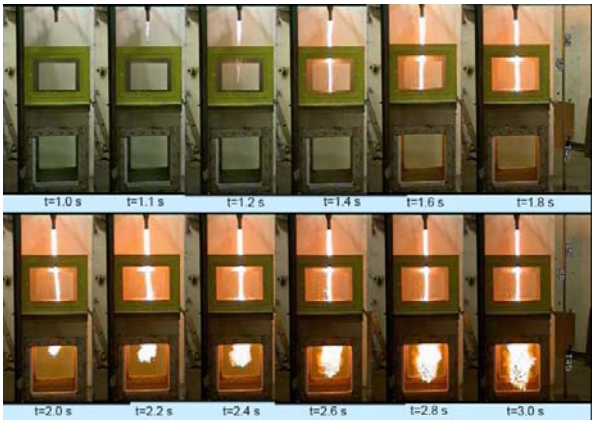

Figure C-2: Initial melt delivery time sequence.

In DEFOR-E experiments DEFOR-03, DEFOR-05 and DEFOR-06 with low subcooling of water, we see that th melt breaks into large particles creating big clusters of debris which are smooth, very brittle and often with hollow cavity. Only few small particles are

found in the bed. The measured porosity of debris bed in DEFOR-03, DEFOR-05 and DEFOR-06 is also quite high (~65%).

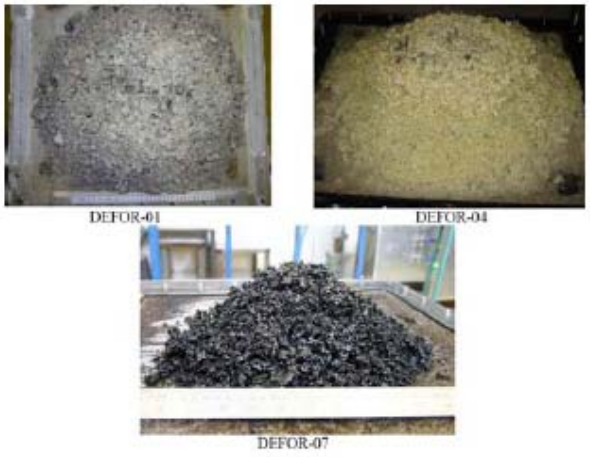

Figure C-3: Debris bed in the highly subcooled water.

Notably, in DEFOR-05 test with low subcooled water temperature and lower pool depth, a 15-cm wide cake was formed at the bottom of the tank (Figure C-4). At the same time we see that no cake is formed in highly subcooled DEFOR-04 which has the same water depth and much higher melt super heat.

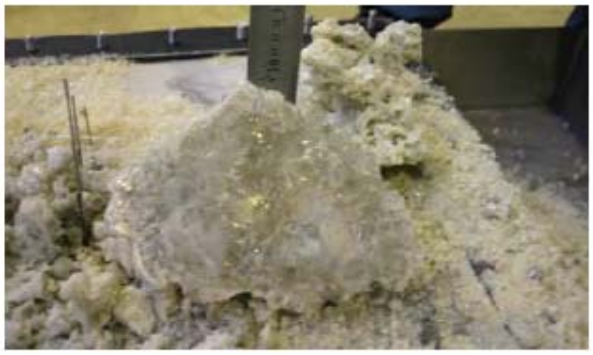

Figure C-4: Cake formation in DEFOR-05 test.

DEFOR-02 Experiment DEFOR-07 Experiment

Figure C-5: Particle distribution in highly subcooled pools.

The melt temperature measured at the centerline nearest to the bottom surface showed that the temperature of the settled debris was higher than Leidenfrost temperature in

DEFOR-05 for a 2 minutes period which is much longer than melt discharging time (~10 seconds).

The shape, size and packing of debris were found to be significantly affected by the coolant temperature and the melt properties. Major fraction of the small particles was found settled at the bottom and the periphery of the heap-like bed in experiments with highly subcooled water. The larger particles were mainly distributed at the top of the bed (Figure C-5).

The effect of melt material type and density on the particles shapes and sizes in experiments with highly subcooled water were investigated. Namely the binary oxide melts were used: glass-type CaO-B_2O_3 with density 2500 kg/m^3 (DEFOR-01, DEFOR-02 and DEFOR-04) and ceramic-type WO_3-CaO with density 6500 kg/m^3 (DEFOR-07). The morphology and sizes of fragments produced in experiments with these two materials was quite different (Figure C-6). Using of more heavy, ceramic-type material leads to reduction of characteristic sizes of particles, debris looks more like sharp rocks. With the lighter glass-type material, the increasing of particle sizes and more smooth particles surface are observed. In the next series of DEFOR experiments we plan to use ceramic-type materials as better corium simulants.

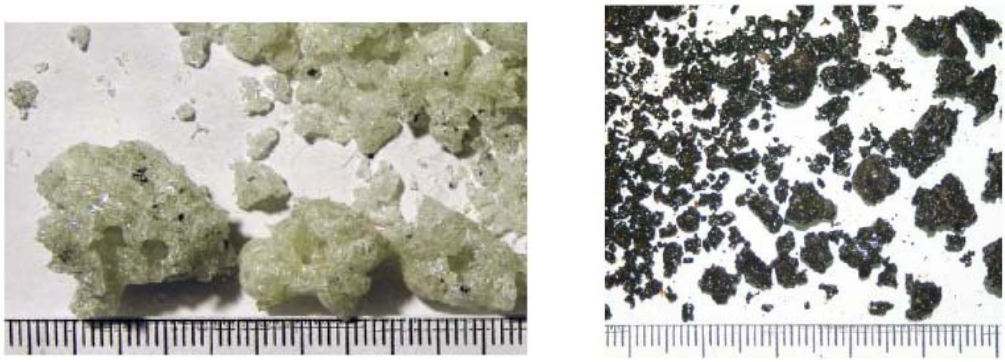

Low dense glass type materials high dense ceramic type materials

Figure C-6: Typical morphology of fragments for high dense ceramic type materials.

2.3.4. Discussion and concluding remarks

The results of DEFOR-E tests generally confirm a conventional view on jet fragmentation, premixing and debris formation processes. Specifically, we observed a strong dependence of debris bed characteristics on water subcooling and pool depth. As the pool depth decreases the debris may reach the bed in a liquid state, rendering an agglomeration and even cake formation. Also, with the decreasing of water subcooling, intense boiling and evaporation was observed, which caused violent mixing in water pool and spreading of melt/debris more uniformly over a larger floor area. Qualitatively, however, the scoping tests were limited by the test section (pool) dimensions so the recirculation flow in the pool was affected by the wall effects.

The DEFOR-E experiments showed that water temperature (subcooling) is one of the most important governing parameters, which has the influence on the jet and particle breakup phenomena, particle sizes distribution, intensity of boiling, heat removal and

characteristics of two-phase flow in debris bed. But the interactions between different physical phenomena during the debris bed formation make it difficult to directly use the DEFOR-E experimental data for prediction of reactor case debris formation processes. That's why we are initiating next series of experiments – DEFOR-S program. The aim of the DEFOR-S program is providing of "Snap-Shot", separate effects experimental study. For this purpose the amount of melt will be reduced to prevent significant increase of coolant temperature during melt poring into the test section pool.

We realize that porosity has the major effect on the coolability of the debris bed. In the coming experiments we will focus our attention on the study of influence of governing parameters on porosity characteristics: *(i)* local characteristics, which mostly depends on particles geometry *i.e*. local porosity, pore sizes distribution, morphology of porosity and *(ii)* macro characteristics, which depends on non-homogeneity and non-isotropy of debris bed formation phenomena i.e. variation of local characteristics on macro scales.

From DEFOR-E study we know that the physico-chemical properties of the melt in addition to the effect of coolant and melt temperatures have the major impact on particles sizes distribution and morphology. The thermal-hydraulic two-phase flow inside porous bed will affect local and macro porosity characteristics.

It is our hypothesis that boiling and steam-water flow will lead to formation of channel-like structures during formation of debris bed. Such channeling of porous debris bed can significantly increase the dry-out heat flux and enhance the coolability of the debris bed. For measurements and quantification of porosity local and macro characteristics as well as channel structures we plan to use 3D computed tomography and porous media inner structure analysis techniques.

To extend the experimental results to reactor scale, a combined approach enclosing experimental, numerical simulation and scaling analysis has to be provided, since *(i)* the experimental work tasks are to provide the quantification of separate-effect phenomena and to build the database for validation and development of closures for semi-empirical models, *(ii)* the scaling analysis task is the extension of laboratory data to reactor scales cases, and *(iii)* the numerical and semi-empirical methods are needed for prediction and quantification of debris bed formation for a given scenario of melt release and pool conditions.

References of Part C

[1] B. W. Spencer, K. Wang et al, "Fragmentation and quench behaviour of corium melt streams in water", NUREG/CR-6133, ANL-93/32, February 1994.

[2] D. Magallon, I. Huhtiniemi and H. Hohmann, "Lessons learnt from FARO/TERMOS corium melt quenching experiments", *Nuclear Engineering and Design*, 189: 223-238 (1999).

[3] D. Magallon, I. Huhtiniemi, "Corium melt quenching tests at low pressure and subcooling water in FARO", *Nuclear Engineering and Design*, 204: 369-376 (2001).

[4] A. Karbojian, W. M. Ma, P. Kudinov, M. Davydov and T. N. Dinh, "A scoping study of debris formation in DEFOR experimental facility", The 15th International Conference on Nuclear Engineering, ICONE15-10472, Nagoya, Japan, April 22-26, 2007.

2.4. *Part D:* A study on ex-vessel debris formation in a LWR severe accident

2.4.1. Introduction

Why to study debris formation in a severe accident ?

In a hypothetical severe accident in a BWR (with core melting, reactor pressure vessel (RPV) failure and subsequent melt discharge to the ex-vessel cavity [1]), long-term coolability of decay-heated core debris and its potential attack on the concrete basemat present a credible threat to the plant's containment integrity. In addressing this challenge, BWR plants in Sweden and Finland adopt cavity flooding as a cornerstone of their severe accident management scheme. Specifically, corium ejected to a highly-subcooled (~80-90K), deep (7-11 m) water pool is expected to fragment, solidify, quench, settle and form a coolable debris bed. The cooling of the debris bed is provided by heat transfer to, and evaporation of, water that ingresses into the porous bed interior from its top or side, with steam generated escaping upwards. The case for coolability of so-formed debris beds is, however, contingent upon a number of parameters, including bed's height, bed porosity and decay heat level among others.

Using the existing data and models for porous bed dryout heat flux, it was shown that the bed coolability may be challenged in various reactor accident scenarios.

Strangely it might seem, while a large number of studies, both computational and experimental, exist on molten fuel-coolant interactions (e.g. jet breakup, melt droplet fragmentation, premixing) very little data and virtually no significant insights were found in the literature on the process of debris bed formation itself. Previous studies of fuel-coolant interactions (FCI) indeed narrowly focused on steam explosion as an imminent threat to the reactor vessel and containment integrity. Even when size distribution of melt fragments was measured by sieving debris beds formed in the FCI experiments, the data were obtained with an objective to help determine melt's interfacial area (needed for heat transfer calculation in pre-mixing), whereas settling and packaging of the debris fragments into a bottom bed were largely overlooked.

The present study aims precisely to fill the above-mentioned gap in contemporary knowledge of severe accident phenomenology. Most importantly, we are motivated by a realization that scattered evidences from previous experiments, both at KTH and elsewhere, readily indicate that in prototypic reactor scenarios, porosity of the ex-vessel debris bed can reach as high as 60%, or even 70%, whereas compact packaging of particles from a batch with a prototypic size distribution renders a porosity of mere 30-35%. Furthermore, results of scoping experiments and analyses in the DEFOR exploratory (DEFOR-E) program at KTH strongly suggest that porous beds formed from a fragmented high-temperature debris is far from homogeneous [2]. Both high porosity and heterogeneity are central to the bed's enhanced dryout heat flux and therefore improved coolability. Consequently, a basic understanding of phenomena that govern debris packaging and bed characteristics is paramount to a reliable prediction of debris bed coolability in reactor accidents.

Scenario and phenomenological feedback

Complexity of the process of debris bed formation is in the feedback interplay of particles formation, sedimentation phenomena and debris bed formation, coolability correspondent phenomena. Particles formation and sedimentation phenomena have direct influence on debris bed formation because the pre-settlement particle temperature and particle size distribution define initial conditions for debris packing. Feedback of debris bed thermal-hydraulics on particles formation, sedimentation, settlement and packing depends primarily on vapor production rate inside the debris bed. Mass flow rate of upstream of hot water/steam is directly proportional to the depth of debris bed and volumetric decay heating. If debris bed is tall enough then it can produce significant amount of steam and change local coolant state.

Qualitatively the details of falling particle – debris bed interrelationship depend on scenario of corium release. From the point of view of debris bed formation, the duration and regime of melt release are the main factors which define characteristic conditions of melt release scenario. The time and regime (coherent jet or dripping) of melt release are the functions of total mass of molten corium and overpressure in the lower plenum, size and shape of vessel rupture. If the duration of corium release from RPV is big enough (due to small size of the vessel failure site, and subsequent low mass flow rate of melt release) for formation of a substantial part of debris bed and establishing global circulation in the pool then we have scenario when new portions of corium is falling into pool with a readily formed and vapor-producing debris bed. For latter portions of the released corium the local coolant conditions can be changed from high subcooled to saturation and even bubbly flow due to decay heating in the debris bed. If the duration of corium release is relatively short (due to a large rupture and/or high melt discharge velocity) and comparable with particle sedimentation time then there is not enough time for the formation of debris bed and consequently for the changes in coolant state due to decay heating and upstream hot water/steam flow from debris bed. But in the last scenario more significant changes in the local coolant state can be achieved due to heat transfer in the dense cloud of falling particles. Higher volume fraction of falling melt debris and consequently higher volumetric heat flux from the falling melt to the surrounding coolant can lead to higher rate of evaporation and voiding in the vicinity of falling debris.

Related experimental evidences

Several studies on jet fragmentation under molten fuel-coolant interaction (MFCI) conditions have been performed in the past using simulant materials as well as prototypic corium as described in the experimental programs CCM [3], KROTOS [4],[5], FARO [6],[7], TROI [8], COTELS [9] and in experimental works performed at NPS-KTH by Haraldson *at all* [10],[11]. In several FARO experiments relevant to ex-vessel MFCI, a cake was found to form at the bottom of the water tank and in other experiment the particles were found to heavily agglomerate. It was also found in FARO experiment (L.31) [12] that there is a stratification of particles with different sizes in different layers of the bed: larger particles at the bottom, smaller on the top. In KROTOS experiments [5] with steam explosion very fine particles were produced and it was suggested that in the

aftermath of an explosion, small particles settled atop of a debris bed may cause reduction of dryout heat flux.

Relatively high porosity (53% … 76%) of debris bed obtained as a result of pouring of melt into water pool was obtained in the previous studies (CCM [2] and FARO [6],[7]) as well as in the last series of DEFOR-E program [1]. In the contrary, random compact packing of the same particles would render a porosity of ~35%. The significantly higher porosity observed in melt experiments may be related to certain order and self organization phenomena in debris packing and formation. The example of influence of order in particulate bed on porosity of the bed can even be found in packing of equal diameter spheres. Random packaging porosity is about 38%. By introducing the order we can obtain 26% porosity for rhombohedral packing and 48% porosity for cubic packing. In DEFOR situation, phenomenological feedback may have been responsible for the ordering and self organization. This hypothesis motivates us to pay a close attention to feedback phenomena.

The results of DEFOR-E tests [2] generally confirm a conventional view on jet fragmentation, premixing and debris formation processes. Specifically, we observed a strong dependence of debris bed characteristics on water subcooling and pool depth. As the pool depth decreases the debris may reach the bed in a liquid state, rendering an agglomeration and even cake formation. Also, with the decreasing of water subcooling, intense boiling and evaporation was observed, which caused violent mixing in water pool and spreading of melt/debris more uniformly over a larger floor area. Qualitatively, however, the scoping tests were limited by the test section (pool) dimensions so the recirculation flow in the pool was affected by the wall effects [2].

Objectives of the present study

The DEFOR-E experiments showed that water temperature (subcooling) is one of the most important governing parameters, which has the influence on the jet and particle breakup phenomena, particle sizes distribution, intensity of boiling, heat removal and characteristics of two-phase flow in debris bed. But complex interactions between different physical phenomena during the debris bed formation make it difficult to extrapolate results of the DEFOR-E and similar integral experiments to reactor scenarios. A new DEFOR-S program was therefore initiated with an objective to obtain data on debris packing and formation under well-defined debris settlement conditions. Within the DEFOR-S program, “Snap-Shot” runs will be carried out to systematically examine different separate effects. Toward this objective, the melt amount used in a test will be reduced to prevent significant increase of coolant temperature and coolant convection during melt poring into the test section pool.
The aim of the present study is to develop methodological basis for DEFOR-S experiments that ensures relevancy of separate effect experimental results to the correspondent prototypic reactor conditions.

2.4.2. Phenomena in debris bed formation

A self-explanatory schematic of multiphase processes involved in debris bed formation is depicted on Figure D-1. Remarkably, one can recognize the “usual suspects”, which have been studied over decades in severe accident research [1], namely molten fuel-coolant

interactions (MFCI) and debris bed coolability (DBC). The debris bed formation appears an in-between step, which therefore is affected by both MFCI and DBC. The phenomena and their feedback are summarized in Figure D-1 and Figure D-2.

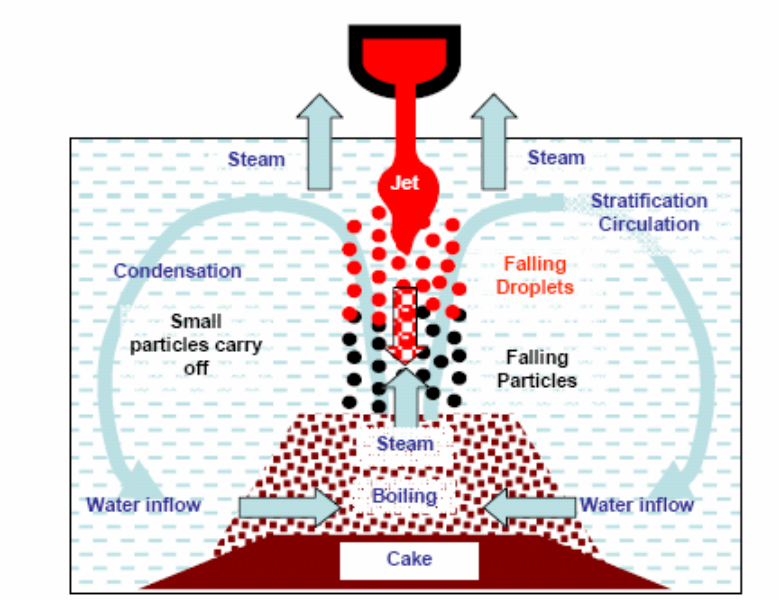

Figure D-1: Phenomena that govern the debris formation.

Based on extensive data, knowledge and insights available from previous studies on MFCI and DBC, one can qualitatively discuss relevant phenomena. Here we limit to highlight aspects which are of particular importance to debris formation.

First, we note that for debris packing prediction, not only averaged particle size but the full particle size distribution is of importance. Both phenomena of jet breakup and sequential droplet fragmentation, in competition with melt solidification (crust formation) at high surface temperature (radiation flux) are known to control the debris size. However, in difference to MFCI analysis, we expect that shape of the debris fragments (some time representing very complex morphology) may greatly affect the debris settlement and packing. Furthermore, whereas in MFCI one is primarily interested in parameters of melt droplets and particles in a pre-mixing zone, for debris formation the whole debris life is relevant. For brittle materials, solidified particles may also fragment at a later stage of sedimentation and packing, that further complicates the quantification of the effect of debris size on debris formation.

Second, and as a consequence of significantly different dynamics of fragments of different sizes, for debris formation one would have to follow separate groups of particles. Notably, in many FCI codes, the small particles and solidified debris are allowed to be “merged” with water since such particles do not participate in the explosion process. For debris formation, small particles must also end up in the debris bed, although they do levitate longer in the pool flow, cooled down and easier to be carried to peripheral regions of the cavity.

Third, given a rather well-known physical picture of MFCI and thermal-hydraulics in debris beds, their interactions are expected to give rise to new behavior. For example, steam production in the decay-heated debris bed promotes two-phase recirculation in the

cavity and increases voiding in the pre-mixing zone. The significance of this effect depends on the pool subcooling, the bed power, the distance between the bed upper envelope and the premixing (jet breakup) zone. Another example of feedback is that the pre-mixing zone causes coolant voiding above the debris bed, promoting the pool overall two-phase natural circulation and hence enhancing coolability of the bottom debris bed.

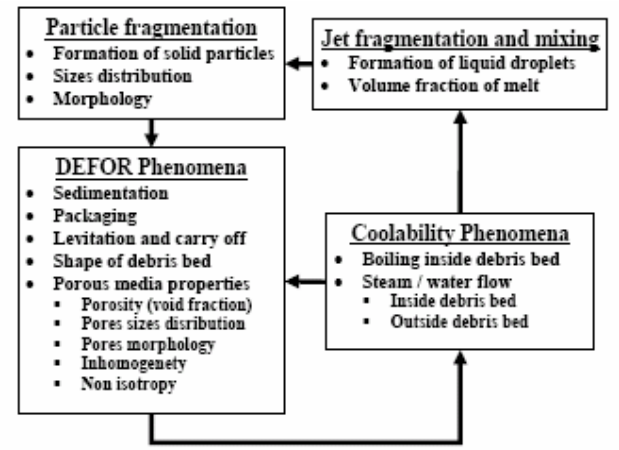

Figure D-2: Debris bed formation phenomena feedback.

2.4.3. Concluding remarks

As practiced in severe accident research, a combination of simulant and/or small-scale experiments, numerical simulation and scaling analysis is necessary to pave way toward understanding reactor-scale phenomena. The experiments can be both either integral or separate-effect. The latter provides a basis for development and validation of closures for semi-empirical models. With respect to debris formation, numerical models for multiphase thermo-hydraulics in the pool and in the debris bed exist and they can be applied for parametric study of processes of importance to debris bed formation. However, no credible models, not to mention a reliable simulation method, exist to describe process of debris settlement, packing and debris bed porosity formation.

Analysis of interrelationships of physical processes involved in debris bed formation during a severe accident in BWR shows that, due to strong feedback between falling debris, coolant and debris bed itself, experimental simulation of the integrated process is not practical within technical constrains and capabilities of small scale laboratory experiments.

For the prediction of prototypic bed properties and consequently coolability of debris bed in reactor scenarios, a combined simulation/experimental approach is a must. A program of critical “snap-shot” experiments named DEFOR-S was defined to enable parametric investigation of debris formation [13]. The role of the snapshot experiments is to obtain data under rather well-defined conditions for use in the development of phenomenological models of debris packing. In near term, the DEFOR-S experiments focus on simulation and study of the influence of steam/water flow inside debris bed and pre-settlement temperature of particles. Based on evaluation of prototypic reactor values of key parameters and scales and taking into account laboratory capability and practical constrains, we formulate a set of technical requirements for “snap-shot” separate effect

experimental program. The DEFOR-S program technical preparation and execution are currently underway and its results will be presented in a forthcoming paper.

References of Part D

[1] T. Okkonen, T. N. Dinh, V. A. Bui, B. R. Sehgal, "Quantification of the ex-vessel severe accident risks for the Swedish boiling water reactors" *SKI Report 95:76*, (1995).

[2] A. Karbojian; W. M. Ma; P. Kudinov; M. Davydov; and T. N. Dinh, "A scoping study of debris bed formation in DEFOR experimental facility", *submitted to 15th International Conference on Nuclear Engineering. Nagoya, Japan, April 22-26,* (2007)

[3] B. W. Spencer, K. Wang et al, "Fragmentation and quench behaviour of corium melt streams in water", NUREG/CR-6133, ANL-93/32, February (1994).

[4] I. Huhtiniemi, D. Magallon and H. Hohmann, "Results of recent KROTOS FCI tests: Alumina *vs*. corium melts", *Proc. of OECD/CSNI Specialists Meeting on Fuel-Coolant Interactions*, Tokai-Mura, Japan, May p.19-21, (1997).

[5] I. Huhtiniemi, D. Magallon, "Insight into steam explosions with corium melts in KROTOS", *Proc. of the 9th Int. Topical Meeting on Nuclear Reactor Thermal-Hydraulics (NURETH-9)*, San Francisco, USA, October 3-8, (1999).

[6] D. Magallon, I. Huhtiniemi and H. Hohmann, "Lessons learnt from FARO/TERMOS corium melt quenching experiments", *Nuclear Engineering and Design*, 189: p.223-238 (1999).

[7] D. Magallon, I. Huhtiniemi, "Corium melt quenching tests at low pressure and subcooling water in FARO", *Nuclear Engineering and Design*, 204: p.369-376 (2001).

[8] J. H. Song, S. W. Hong et al., "Insights from the recent steam explosion experiments in TROI", *J. Nuclear Science and Technology*, 40 (*10*): p.783-795 (2003).

[9] M. Kato, H. Nagasaka et al, "Fuel coolant interaction tests under ex-vessel conditions", *Proc. of the OECD workshop on ex-vessel debris coolabilitty*. Karlsruhe, Germany, (1999).

[10] H.Ó. Haraldsson, H.X. Li, T.N. Dinh, J.A. Green and B.R. Sehgal, *"*Hydrodynamic fragmentation of molten metal jet in water: Effect of melt solidification and coolant voiding*",* Twelfth Proceeding of Nuclear Thermal Hydraulics, American Nuclear Society (ANS), New Mexico, USA, October p.16-20, (1995).

[11] H.Ó. Haraldsson, and B.R. Sehgal, *"*Effect of subcooled liquid coolant on particle size generated during fuel coolant interactions*",* The Ninth International Conference on Nuclear Reactor Thermal Hydraulics, san Francisco, California, USA, October p.3-8, (1999).

[12] I. Huhtiniemi, D. Magallon, *"*Insight into steam explosions with corium melts in KROTOS*"*, Proc. Of the 9th Int. Topical Meeting on Nuclear Reactor Thermal-Hydraulics (NURETH-9), San Francisco, USA, October p.3-8, (1999).

[13] P. Kudinov, A. Karbojian, W.M. MA, M. Davydov and T.N. Dinh, "A study of ex-vessel debris formation in a LWR severe accident", International Conference on Advances in Nuclear Power Plants, ICAPP-2007, Nice, France, May 13-18, 2007

2.5. *Part E:* Coolability of a bottom-fed debris bed

2.5.1. Introduction

Since coolability of corium debris beds is of paramount importance to the stabilization and termination of a severe accident, debris bed coolability has been studied over the years. In the past, study of debris bed coolability was focused on top-flooding scenarios, which manifest situations when side and bottom coolant injection are assumed to be negligible or absent, for example when corium debris is spread evenly over the cavity floor. Numerous analytical and experimental investigations were concerned with understanding and prediction of the dryout heat flux (DHF) which is the maximum heat flux that can be removed from a debris bed by the coolant inflow. For a uniform debris bed packed by spherical particles, the dryout heat flux can be determined by counter-current flow limit (CCFL) and predicted, with a fair accuracy, by analytical models of Lipinski type and its variations [2-3].

Given reactor scenarios with formation of deep beds or fine beds with either small particles or low porosity, the existing models predict that the top-flooding is insufficient to remove decay heat released in such debris beds. This perception has motivated further search for additional means to enhance debris bed coolability, eventually benefiting reactor safety performance.

In prototypic reactor scenarios, the debris beds formed from fuel-coolant-interaction (FCI) are more likely to have a heap-like shape (see Figure E-1), which allows coolant ingression from the sides as well as from the top, thus improving coolability of the bed's peripheral region. In preferable cases, it was suggested that the bed coolability can be further enhanced by providing coolant bottom feeding. In such a situation, the coolant will heat-up and boil due to the heat transfer from the decay-heated debris. The porous bed is therefore filled with two-phase mixture, whose density is significantly lower than the water density. Consequently, a gravity head difference between the liquid outside the bed and the two-phase mixture inside the bed will drive the coolant into the bed interior, forming a natural circulation loop, as shown in Figure E-1. This cooling scheme is called Natural Circulation Driven Coolability (NCDC).

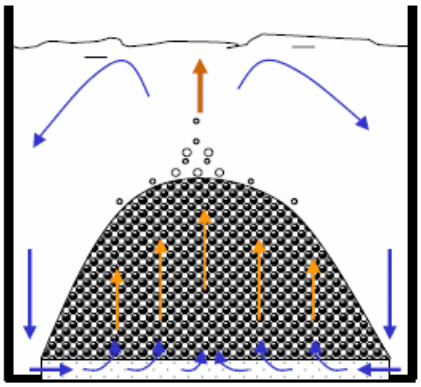

Figure E-1: *Debris bed with coolant bottom-fed*

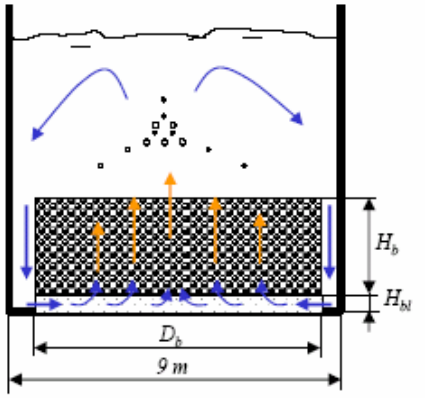

Figure E-2: *Schematic of a* simplified *ex-vessel debris bed with coolant bottom-fed.*

In practice, coolant inflow through the bed's bottom, can be facilitated by means of a retrofit device (downcomer, distributor embedded on cavity floor) or a "wet" core catcher in new designs, or even "naturally" by a porous decay-heat-free bottom layer, formed as a result of earlier discharge of metallic melt (e.g. steel).

Motivated to enhance the coolability of debris bed, several experimental investigations were conducted for bottom-fed debris beds, including bottom forced injection and downcomer installation [1,4-6]. However, the physical picture remains fragmentary, rendering questions in applicability of the experimental results to plant conditions. There is a clear need for analytical work which would bridge experiments to understanding of processes in NCDC and their safety implications.

The present study employs an analytical approach to calculate characteristics of two-phase thermal-hydraulics in porous media. Verification of the model is performed against POMECO data. The friction law (Lockhart-Martinelli correlations) employed in the present model was also validated against data from packed-bed reactors and micro-channels found in the literature [7]. Thus, we believe the model prediction can give insights for debris bed coolability with an acceptable error. We then use the model to evaluate efficacy of natural circulation driven coolability (NCDC) of debris beds formed ex-vessel in hypothetical severe accident scenarios of a BWR.

2.5.2. Analytical Model

Although there exist numerous tools for description and prediction of two-phase flow in porous media, including multi-dimensional codes, in this study we choose to develop and apply a simple and robust semi-analytical 1D treatment, which enables us to effectively perform parametric study of debris bed coolability over a broad range of conditions.

Notably, two-dimensional simulation of debris bed flow presented in our study in the paper [8] shows that coolant flow in bottom-fed debris bed is indeed dominantly one-dimensional with negligible radial velocity component.

The governing equations for coolant flow in the debris bed are derived from mass, energy and momentum balance. The detailed description of the equations can be found in [9]. We apply the well-known Lockhart-Martinelli approach [10] for two-phase flow frictional pressure drop:

$$\frac{dp_f}{dz} = \left(\frac{dp}{dz}\right)_l \cdot \phi_l^{\,2} = \left(\frac{dp}{dz}\right)_v \cdot \phi_v^{\,2} \qquad \text{(E-1)}$$

where $\left(\frac{dp}{dz}\right)_l$ and $\left(\frac{dp}{dz}\right)_v$ are single-phase pressure gradients of liquid and vapor, respectively, which are calculated by the Ergun's equation [11]. The liquid Martinelli multiplier $\phi_l^{\,2}$ is defined as

$$\phi_l^{\,2} == 1 + \frac{C}{X} + \frac{1}{X^2} \qquad \text{(E-2)}$$

where C is a constant determined by experimental data, and X is Martinelli parameter [10]. For isothermal two-phase flow, constant C is determined for different flow regimes

[10]. For boiling two-phase flow in a channel, Martinelli-Nelson suggested using one value for all turbulent regimes (i.e. C=20).

2.5.3. Results and analysis

Model Verification

Lockhart-Martinelli approach was developed for two-phase flow in pipes. In chemical and process engineering, the approach has also been used to analyze tricked bed reactors (downward flow) and flooded-bed reactors (upward flow) [7]. For example, Larachi et al [7] compared the prediction of the approach with 3400 experimental data points obtained from various packed beds flooded by different liquid and gas, and found an acceptable agreement. However, for a lower flow velocity range which is the case for the NCDC, the prediction appears to underestimate the flow resistance. In addition, coolant boiling due to the bed internal heating may increase resistance in corium debris beds.

The advantage of Lockhart-Martinelli approach is convenient to use in design analysis with an acceptable accuracy. The method is also easy to validate and adjust by using experimental data and choosing appropriate value for constant C in Eq.E-2.
In the present work, we chose the data of a particle bed in a POMECO test [1] to determine the C value. The bed is composed of sands with mean particle size of 1mm. The bed porosity of 0.36 was measured. Electric heaters were uniformly embedded in the bed to provide internal heating. The particle bed is sitting on a perforated plate which is 50mm above the water pool bottom. A pipe with 50mm inside diameter is placed in the middle of the debris bed to serve as a downcomer of water flow.

If C=30, the predicted dryout heat flux in the bed is around 351 kW/m^2 which is comparable with value of 331 kW/m^2 measured in the experiment. Notably, the result of this 1D model coincides with that calculated by the WABE-2D code [8].

Reactor Application

Hereafter the model is applied to the coolability analysis of ex-vessel debris beds formed in hypothetical severe accident scenarios of a boiling BWR which has thermal power of 2500 MW and the cavity diameter of $9\ m$ (see FigureC-2). It is assumed that the maximum mass of an ex-vessel corium debris bed is about 180 tons, with the average corium density of 7660 kg/m^3.

The dryout heat flux is fixed for a top-flooding bed with the known particle size and porosity, since the capability of decay heat removal is only related to the top surface area of a bed. However, for a bottom-fed bed, the decay heat removal also depends on the bed height as well as surface area. Thus, heat density (heat per unit volume) will be used in the following study. The critical heat density when dryout occurs is called dryout heat density (DHD) accordingly. For uniformly heated beds, DHD is related to the widely-used dryout heat flux (DHF) as DHF = DHD·H_b, where H_b is the height of the decay-heated debris bed.

In total, 5 cases were analyzed to investigate the effect of different debris bed characteristics and flow resistance correlation on the coolability (dryout heat density). In

all cases, the debris mass and density are taken the same as 180 tons and 7660 kg/m^3. The decay-heat-free bottom layer is assumed to have the thickness of 0.1 *m* in all cases.

Case 1 has a debris bed spreading over 8.5 *m* diameter, so that there is a 0.25 *m* gap between the cavity wall and the bed, which serves as a downcomer in the NCDC configuration. The particle size d_p and porosity ε are 3 *mm* and 0.4, respectively. When increasing heat load in the bed, the exit vapor quality will also increase [9], but the temperature remains at saturation prior to dryout. In this case, the dryout (maximum vapor quality x=1) occurs at heat density of 3.15 MW/m^3, at which the temperature excursion occurs. This dryout heat density is much higher than 1.3 MW/m^3 of a top-flooding bed predicted by Reed's model [1].

Case 2 is to investigate the effect of debris bed height on the coolability, when keeping the bed mass, porosity and particle size fixed. In this case, the bed diameter decreases with increasing height (Figure E-3a). From Figure E-3b, it can be seen that dryout heat density of a bottom-fed bed is much higher than that of a top-flooding bed, even for a deep debris bed. If the bed height is 2 meter, for instance, the DHD of top-flooding bed is only 0.45 MW/m^3, whereas the DHD of bottom-fed bed is 1.11 MW/m^3. It is observed that when the bed height increases from 0.69 m to 2 m, the DHD increases by the factor from 141% to 146% in comparison with top-flooding bed.

In Case 3, the effect of the bed porosity on the dryout heat density is investigated (see Figure E-4). When the particle diameter is kept unchanged (d_p=3 mm), the dryout heat density will increase with the increase of porosity, which is similar behavior in a top-flooding bed. In the bottom-fed beds, the gain of dryout heat density under an increased porosity appears more significant than that in top-flooding beds. It appears that the DHD increases by the factor from 100% to 160% in comparison with top-flooding bed, when the porosity increases from 25% to 65%.

The particle size also significantly affects the coolability of debris bed. As shown in Figure E-5 (for Case 4), the particle diameter on the dryout heat density is found to have a similar influence as bed porosity. When the porosity is fixed (ε=0.4), the dryout heat density will increase as the particle diameter increases. For the bottom-fed beds, the influence of particle size is profound. It appears that the DHD increases by the factor from 82% to 165% in comparison with top-flooding bed, when the particle size increases from 1mm to 6mm.

In Case 5, we examine a stratified bed with coolant bottom feeding. The debris bed in Case 5 is comprised of 0.3m-thick layer with 1mm particles sit atop of a 0.39m thick layer with 3mm particles. The dryout heat density of the bed is 1.22kW/m^3 by prediction, which is much lower than that of Case 1 which has the same particle size in the lower layer. However, the DHD in bottom-fed beds is almost twice larger than that of the top-fed bed. Clearly, the NCDC fosters an enhancement also in stratified beds.

In the present study we use a bigger value for C (C=30) in Eq.E-2 than the "classical" value used in Martinelli-Nilsson correlation (C=20) for two-phase flow in pipes. Our choice is based on benchmarking the model against POMECO test data and the WABE code calculation. To quantify the sensitivity of this choice, we examine the effect of C value on the predicted dryout heat density [9]. It is shown that the dryout heat density is

reduced by a mere 12% when the C value increases from 20 to 30. Such a discrepancy is well within the acceptable range of uncertainty considered for this type of study.

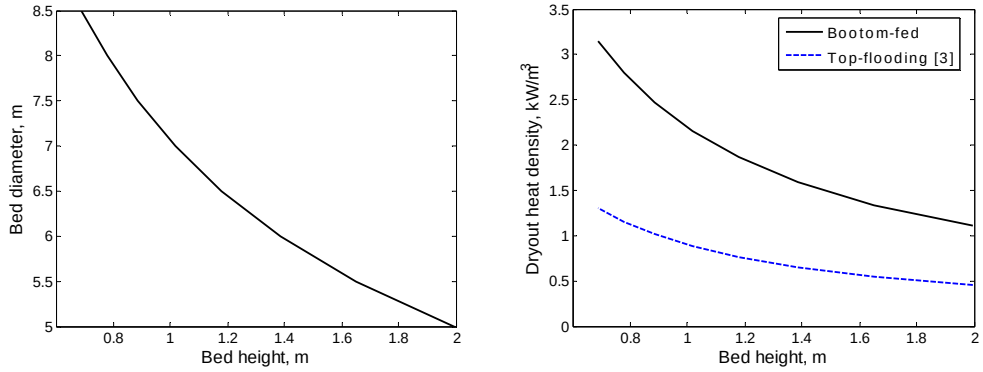

(a) (b)

Figure E-3: *Bed diameter and dryout heat density as function of bed height.*

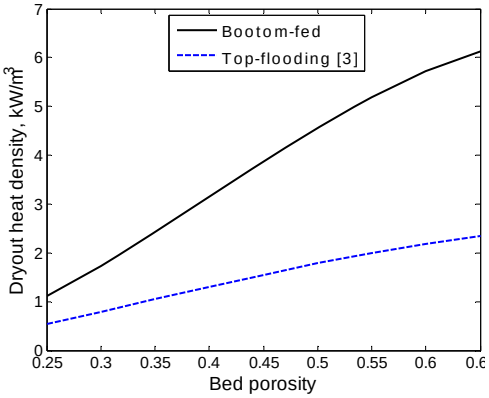

Figure E-4: *Dryout heat density variation with bed porosity.*

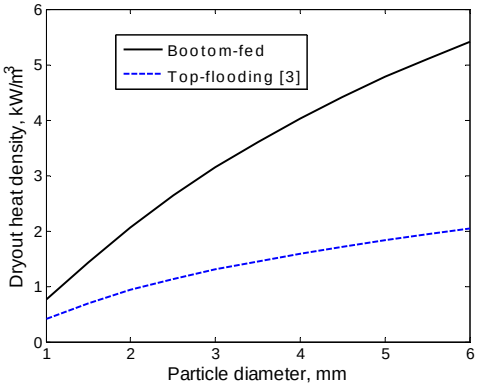

Figure E-5: *Dryout heat density variation with particle size.*

3.5.4. Conclusions

An analytical model was developed, validated and used to compute characteristics of two-phase thermal-hydraulics in the debris beds. The model makes use of the Lockhart-Martinelli approach for calculation of two-phase flow resistance in porous media. The approach is very convenient to represent and analyze different experimental configurations and device designs. The model used is validated against the POMECO experimental data and the WABE code result.

We use the developed model to investigate Natural-Circulation-Driven-Coolability (NCDC) of debris beds with coolant bottom-feeding. The coolability enhancement is quantified through the evaluation of the bed's dryout heat density, in comparison with the dryout heat flux predicted by Reed's model [1] for top-flooding beds. From the analysis of ex-vessel debris bed coolability, the following conclusions can be drawn:

- The coolant bottom-fed is proved to be an effective avenue to enhance debris bed coolability. For instance, the dryout heat density with the NCDC is 140% higher than that of top-flooding bed, if the bed has 40% porosity, 3mm particle size and a high-porosity decay-heat-free bottom layer.
- The comparative enhancement of the dryout heat density in the NCDC increases with the increase of bed porosity and particle size.
- For a stratified bed with a fine particle layer sitting atop another debris layer, the dryout heat flux is also elevated due to the NCDC. The coolability enhancement is up to 100%.
- Water subcooling helps increase the dryout heat density, but the effect is counter-acted also by the reduced driving head due to steam condensation above the bed and decreases with the pool heatup in long term.
- Given a decay-heat-free bottom layer with the same porosity and particle size as the main debris bed, the dryout heat density remains higher than that of the top-flooding bed. The coolability enhancement is up to 100%.
- In general, the dryout heat density is predicted to increase by a factor of 80% to 160% due to NCDC, depending on bed configuration and characteristics.

References of Part E

[1] M. J. Konovalikhin, "Investigations on melt spreading and coolability in a LWR severe accident", *Ph. D thesis of Royal Institute of Technology*, Stockholm, November 2001.

[2] R.J. Lipinski, "A coolability model for post-accident nuclear reactor debris", Nulcear *Technology*, **65**: 53-66 (1984).

[3] A.W. Reed, "The effect of channeling on the dryout of heated particulate beds immersed in a liquid pool", *PhD thesis of Massachusetts Institute of Technology*, Feb. 1982.

[4] K.H. Bang et al, "Enhancement of dryout heat flux in a debris bed by forced coolability flow from below", *Proc. of NURETH-11*, Aavignon, France, Oct. 2-6, 2005.

[5] G. Hofmann, "On the location and mechanisms of dryout in top-fed and bottom-fedparticulate beds", Nuclear Technology, Vol. 65 (1984).

[6] M. Miscevic at al., "Experiments on flows, boiling and heat transfer in porous media: Emphasis on bottom injection", *Nuclear Engineering and Design*, **236**: 2084–2103 (2006).

[7] F. Larachi et al., "Two-phase frictional pressure drop in flooded-bed reactors: A state-of-the-art correlation", *Chem.* **21**(11): 888-893 (1998).

[8] W.M. Ma, M. Buck, M. Bürger and T.N. Dinh, "Analysis of inhomogeneity effect on debris bed coolability", *Proc. of the 15th International Conference on Nuclear Engineering*, ICONE15-10472, Nagoya, Japan, April 22-26, 2007.

[9] W.M. Ma and T.N. Dinh, "Coolability analysis of bottom-fed debris beds in severe accidents", The 15th International Conference on Nuclear Engineering, ICONE15-10472, Nagoya, Japan, April 22-26, 2007.

[10] G.B. Wallis, *One-dimensional two-fhase flow*: McGraw-Hill, 1969.

[11] S. Ergun, "Fluid Flow through Packed Columns", *Chemical Engineering Progress,* **48** (2): 89-94 (1952).

2.6. *Part F:* Analysis of the effect of debris bed inhomogeneity on its coolability

2.6.1. Introduction

It is noted that previous analyses of debris bed coolability in a reactor accident have largely assumed that debris beds are homogeneous and uniformly spread over the pool bottom. Characteristics of such a homogeneous bed include a volume-averaged porosity and mean particle diameter (traditionally taken from a particle sizes distribution obtained in FCI tests through a sieving technique). Thus, neither the prototypic bed's porosity nor its interior structure (e.g. pore size distribution) has been accurately reproduced in the previous experimental and analytical studies. In our view, bed characteristics and its coolability are affected, to a significant extent, by (i) intense boiling on high-temperature corium fragments on debris packing during bed formation, (ii) bed inhomogeneity, (iii) history effect of bed formation on bed cooling dynamics (quenching), (iv) bed's three-dimensionality, and (v) heat source distribution.

In this work, we focus on the potential impact of bed inhomogeneity on debris coolability, namely the effect of bed's micro and macro heterogeneity (in term of particle size and pore distributions in space) is examined. A vehicle for this analysis is WABE-2D code developed at IKE-Stuttgart University for simulation of two-phase thermal-hydraulics in debris bed. The code description and validation against experimental data can be found in [1-2].

The present analysis is performed for two types of "unit volume": *i)* one is called macro bed with 350mm diameter that incorporates either a channel or a surrounding high porosity ring, representing macro-heterogeneity; *ii)* another is called mini bed with 50mm diameter that incorporates a high-porosity column in the bed's middle, representing micro-heterogeneous bed.

2.6.2. Results and analysis

Code Verification

As mentioned above, the WABE-2D code was extensively validated against experimental data [1-2]. As a further verification, in the present study the WABE-2D code was used to examine thermal-hydraulics of a particle bed in a POMECO test [3]. The bed is composed of sands with mean particle size of 1mm. The bed porosity of 0.36 was measured. Electric heaters were uniformly embedded in the bed to provide internal heating. The particle bed is sitting on a perforated plate which is 50mm above the water pool bottom. A pipe with 50mm inside diameter is placed in the middle of the debris bed to serve as a downcomer of water flow. The bed configuration and dimensions are as shown in Figure F-1.

Due to the axisymmetric geometry, only half of the bed on the right side is used in the calculation, and water is assumed to be saturated. Figure F-2 shows the profile of liquid velocity and particle temperature in the debris bed. It is observed that the liquid water enters the bed mainly through the downcomer into the bottom gap. The water which

entered the bed bottom starts evaporation and two-phase mixture takes place in the bed. The gravity head difference between the downcomer and the particle bed provides a driving force for natural circulation, which alleviates the severe counter-current flow limitation in a top-flooding bed and therefore enhances the coolability. We call this regime a Natural-Circulation-Driven Coolability (NCDC), to differ from counter-current flow coolability. Notably, in such beds with downcomer, the flow is dominantly one-dimensional and concurrent (see velocities of liquid in Figure F-2), which means a one-dimensional assumption in an analytical model [4] is reasonable for such a bed.

The dryout begins from top layer of the bed, which is different from top-flooding bed which starts dryout from bottom. The prediction of dryout heat flux in the bed is around 351 kW/m^2 which is 6% higher than the value of 331 kW/m^2 measured in the experiment. The result is quite acceptable given assumptions used in simulation and evaluation of bed's two-phase thermal-hydraulics. In other words, the WABE prediction is comparable with the POMECO experimental data.

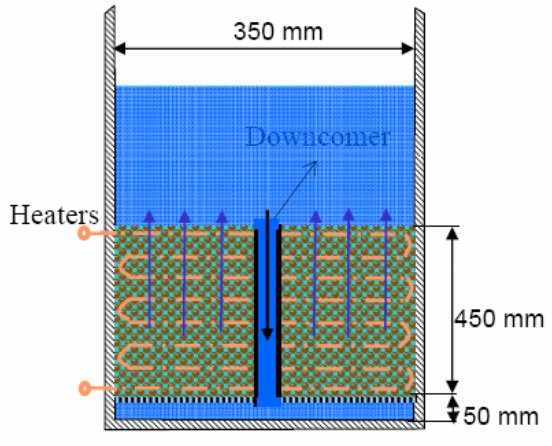

Figure F-1: *Schematic of a POMECO test* with 30mm I.D. downcomer [3]

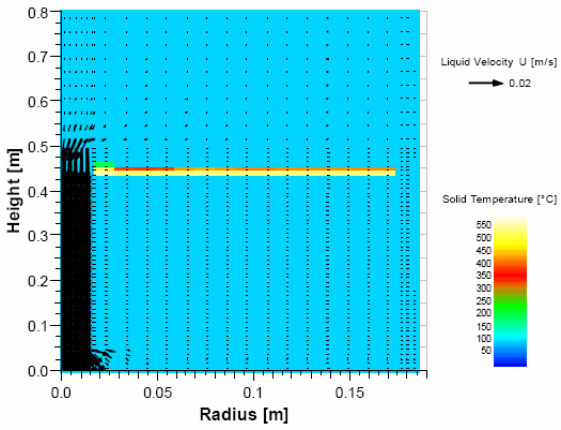

Figure F-2: *Profile of liquid velocity and particle temperature.*

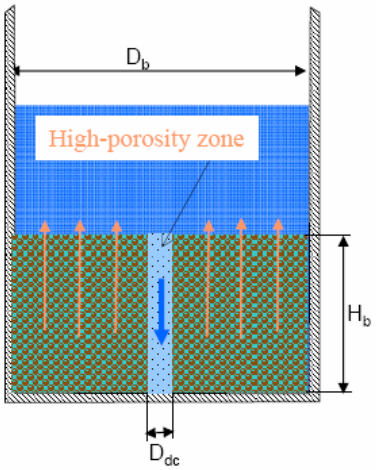

Figure F-3: Debris bed with inhomogeneity in porosity and particle size.

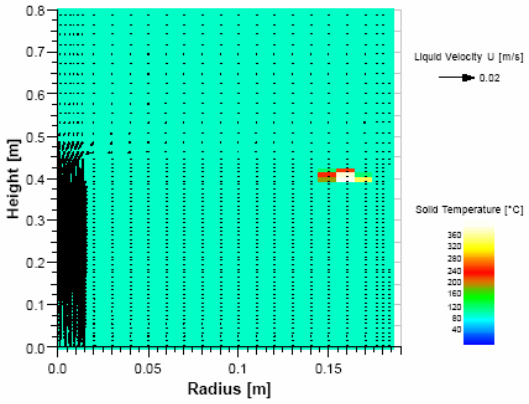

Figure F-4: Post-dryout of a top-flooding bed in Case 1 (heat load =345 kW/m^2).

Inhomogeneity Effect on DHF

In the present study, the bed inhomogeneity is represented by a channel or a high-porosity zone in the base bed, as illustrated in Figure F-3. The basic configuration is composed of particles of 1mm diameter, and has porosity of 0.36. Thus, the dryout heat flux obtained from above-analyzed top-flooding bed can serve as the baseline for comparison in the following study.

Total 6 debris beds are investigated here (see Table F-1), where two types of unit volume and respective macro and micro inhomogeneity are represented: *i)* so-called macro bed with 350mm diameter that incorporates either a channel (Case 1) or a surrounding high porosity ring (Case 2); *ii)* so-called mini bed with 50mm diameter that incorporates a high-porosity column in the bed's middle (Case 3 ~ Case 6). The prototypical debris bed may consist of many such macro and mini beds. In all cases, we call the channel and high-porosity zones as 'downcomer', since they provide a similar function of downcomer in a traditional natural circulation loop.

Table F-1: Calculation matrix

Case	***Bed***				***Downcomer***			
	d_p (*mm*)	ε (/)	D_b (*mm*)	H_b (mm)	d_p (*mm*)	ε (/)	D_{dc} (mm)	**heating**
1	1.0	0.36	**350**	450	100	0.8	30	*No*
2	1	0.36	**250**	450	3	0.4	250-350	*Yes*
3	1.0	0.36	**50**	450	3	0.6	10	*Yes*
4	1.0	0.36	**50**	450	1	0.6	6	*Yes*
5	1.0	0.36	**50**	450	2	0.72	6	*Yes*
6	1.0	0.36	**50**	450	1	0.6	10	*Yes*

In Case 1 the bed embeds a downcomer-like channel in the middle. The configuration is different from the POMECO bed mentioned above, by the fact that there is no gap under the bed and no wall for the channel. Thus, the water will enter the downcomer, and radially permeate to the bed body along the bed height, as shown in Figure F-4. Due to a numerical limitation (for 100% porosity), in the calculation the channel is defined to have 100mm particle diameter and 0.8 porosity, which yields an around 28 mm hydraulic diameter.

In this case, the dryout was found to first occur at the upper-right corner of the bed. This is because of the biggest resistance for the liquid to reach to that corner due to evaporation depletion and upward vapor flow. One of the main different results of the case from the bed with bottom gap (as POMECO test) is that the horizontal velocity of liquid is appreciable here.

The dryout heat flux of the bed in Case 1 is $328 kW/m^2$ as predicted by WABE-2D code. The value of dryout heat flux is 44% higher than that predicted for top-flooding

bed ($228 kW/m^2$). This confirms the positive effect on coolability in a debris bed with a porous channel within.

In Case 2, the bed is surrounded by a larger scale, high-porosity ring. In this case, the outer ring is expected to serve as a downcomer, and coolant is transported to the inner bed. In this case, vapor generation occurs in the outer ring due to the bed's decay heat, inducing a counter-current flow in this region. However, the process is dominated by excessive water ingression into the outer ring and towards the inner ring. As a result, the dryout onset of the inner ring is delayed, compared with the only top-flooding situation of the inner ring. The dryout heat flux is predicted to be 325 W/m^2, which is 43% higher than that of top-flooding bed of the inner ring.

In Case 3, we consider a unit volume of a 50-mm-diameter mini bed with a high-porosity zone in the unit's middle. The unit is representative of a small part in a large bed. The unit's inner zone contains a 10mm cylindrical column with 3mm particles and 60% porosity. The volume ratio of the inner zone to the whole bed (unit) is 4%. In this case, the high-porosity zone is too found to serve as a downcomer for the remaining part of the bed. The dryout heat flux is enhanced by 48% in comparison to the top-flooding bed.

It should be noted that if we consider a uniform bed with an average porosity and particle size, the predicted dryout heat flux would be nearly identical to that of the top-flooding, since the inner zone contribution is minute that it does not alter the average porosity and particle size to any significant extent. In other words, a mini channel or micro-heterogeneity (high-porosity) zone in a debris bed would not be easily recognized from the bed-averaged porosity measurement, yet such mini-channels are capable of dramatically changing the coolant ingression mode, and eventually improving the dryout heat flux.

The effect of such micro inhomogeneity on dryout heat flux is a finding of the present work, as it has not been addressed in the coolability study performed in the past.

In Case 4, we ask the question what would happen if the high-porosity zone is reduced and has the same particle size as the main bed.. We assume a bed with a mini channel of 6mm diameter and made of 1mm particles. The dryout heat flux predicted by the code is 242 kW/m^2 that has 6% gain in DHF comparing with the top-flooding. If the particle size and porosity increase to 2mm and 0.72, respectively, while keeping micro-channel diameter fixed (Case 5), the increase in the dryout heat flux is 21%. The similar percentage of the DHF gain is obtained for Case 6 where the particle size and porosity are kept the same as Case 4, but the micro-channel diameter increase to 10mm.

The values and gain percentage of dryout heat flux for all 6 Cases are listed in Table F-2.

The analysis result suggests existence of a threshold for the downcomer size, porosity and particle size. If the downcomer diameter is less than 6mm for a bed in Case 4, for instance, the increase in dryout heat flux becomes insignificant. The decrease in porosity and particle size in the downcomer also lead to reduced DHF. Such behavior

is understandable, since the dryout heat flux is actually determined by competition of coolant inflow in the downcomer and the remaining bed. Thus the key is flow resistance. If the flow resistance in the downcomer is sufficiently low, then excessive water becomes available to the remaining part of the bed, and the dryout heat flux would be improved. The lower the resistance in the downcomer is, the higher the dryout heat flux is. As the resistance in the downcomer becomes negligible in comparison with the bed's resistance, the dryout heat flux no longer increases. On the other hand, if the downcomer's size is decreased, its effect on coolability may disappear after a threshold, which understandably depends on porosity and particle size.

Table F-2: Dryout heat flux

Case	Inhomogeneity	*DHF (kW/m2)*	*DHF/DHF$_{top}$**
1	Macro	328	44%
2	Macro	325	43%
3	Micro	338	48%
4	Micro	242	6%
5	Micro	276	21%
6	Micro	276	21%

* DHF_{top} is *228 kW/m^2* for the top-flooding bed.

Implication on Coolability

The implications of the above findings on debris bed coolability are straightforward. Both macro-inhomogeneity and micro-inhomogeneity serve as potential avenues for enhancing debris bed coolability in prototypic reactor situation. Notably, the prototypical debris bed in a severe accident can be viewed as an assembly of unit volumes considered in preceding sections. A macro bed may compose of a group of mini beds. Although the downcomer (channels or high-porosity zones) only occupies a relatively small fraction (say, 4%) of the total volume of the whole bed, their contribution to dryout heat flux is significant. Remarkably, such coolability enhancement could not be predicted by the treatment of uniform bed with mean porosity and particle size.

Analysis of preliminary data on debris bed formation suggests that the debris bed is likely to be heterogeneous, both macroscopically and microscopically (in definitions used in the present work). The present study motivates and provides guidance for DEFOR program in its effort to quantify and predict bed characteristics which are of importance for the assessment of bed coolability.

2.6.3. Conclusion and perspective

The present study focuses on the effect of bed inhomogeneity on coolability. The authors are not aware of similar effort reported in the open literature. Two-types of "unit volumes" that represents macro-heterogeneous bed and micro-heterogeneous bed are considered. The WABE-2D code is used as a vehicle to analyze two-phase thermal-hydraulics in debris bed, and predict the dryout heat flux.

Based on the analyses and result, the following conclusions can be drawn:

- The downcomer-like macro channel in a macro bed plays an important role in determine dryout heat flux, even it's the downcomer volume constitutes a small volume fraction (<1%) of the whole bed. In the cases chosen, the dryout heat flux is predicted to be 44% higher than in a top-flooding uniform bed with average porosity and particle size.
- Presence of small-scale high-porosity zones in a bed, even at small volume fraction (<4%) is predicted to increase the dryout heat flux by up to 48% comparing with the top-flooding bed.
- Remarkably, high-porosity zones are so small in volume fraction that their contribution to the average bed characteristics is negligible, while their effect on bed coolability is significant.
- There appears a threshold size of the high-porosity zone, under which the increase in dryout heat flux become marginal.
- We believe a prototypical debris bed comprises of various macro-bed configurations which in turn are composed of mini beds.
- Such micro and macro inhomogeneity are lost in previous bed-average treatments. It remains of importance that the impact of inhomogeneity on coolability is further scrutinized, confirmed and quantified using a multi-dimensional simulation. Eventually, the effect of bed inhomogeneity must be factored in a bed-averaged treatment.

References of Part F

[1] M. Bürger, M. Buck, W. Schmidt and W. Widmann, "Validation and application of the WABE code: Investigations of constitutive laws and 2D effects on debris coolability", *Nuclear Engineering and Design*, **236**: 2164–2188 (2006).

[2] W. Schmidt, "Influence of multidimentionality and interfacial friction on the coolability of fragmented corium", *Ph. D thesis of University of Stuttgart*, May 2004.

[3] M. J. Konovalikhin, "Investigations on melt spreading and coolability in a LWR severe accident", *Ph. D thesis of Royal Institute of Technology*, Stockholm, November 2001.

[4] W.M. Ma and T.N. Dinh, "Coolability analysis of bottom-fed debris beds in severe accidents", *Proc. of the 15th International Conference on Nuclear Engineering*, ICONE15-10472, Nagoya, Japan, April 22-26, 2007.

2.7. *Part G:* Dynamics and preconditioning in a single drop vapor explosion

2.7.1. Introduction

Vapor explosion may occur during a relocation of a molten material at high temperature into a pool of volatile coolant such as in a severe nuclear reactor accident [1,2]. Phenomena of vapor explosion have been studied by many researchers over the past several decades, both experimentally and theoretically. Experiments to characterize micro-interactions in steam explosion were performed using a high speed video camera [6] and a flash X-ray imaging of melt droplet under a very strong shock wave [4], as well as under a weak pressure impulse [5] to trigger the interaction. Unfortunately, the use of flash X-ray systems, which provides only one snapshot image during each test, unable to acquire a consistent sequence of entire vapor explosion processes. Notably, due to the intensity and microscopic scale of processes of importance it has been very difficult to obtain data on micro-interactions for the basic understanding. A mechanistic treatment of micro-interactions remains elusive. In this study, micro-interactions in a droplet explosion are studied by using a novel diagnostic technique developed at KTH. The system, named SHARP (Simultaneous High-speed Acquisition of X-ray Radiography and Photography) is designed to enable synchronized visualization of both bubble dynamics and melt evolution during the explosion period. Our plan is to start with tests with a weak pressure wave (characteristic of triggering) and later move on to tests with a strong pressure wave (characteristic of detonation regime). The tests should cover a range of corium simulant materials, from tin and medium-temperature oxidic melts and later also high temperature metal and ceramic oxide materials. The objectives of the present experimental program on droplet explosion are dual. First, we aim to obtain high-quality experimental data in well-controlled experiments. Such data are useful for the development and validation of mechanistic models, including CFD-based simulation methods. Second, the data are processed to establish behaviors which provide new insights into the physics of micro-interactions. In the present study, we focus on the second objective.

2.7.2. MISTEE test facility

A test facility, called **MISTEE** (**M**icro **I**nteractions in **S**team **E**xplosion **E**xperiments) as shown in Figure G-1a is used to perform single drop experiments which are dedicated to pursue a basic understanding of micro-interactions in vapor explosion. The test facility consists of a test chamber, a melt generator, an external trigger system, an operational control system, a data acquisition and the visualization system. The test section is a rectangular Plexiglas tank (180x130x250mm) where a piezoelectric pressure transducer is flush-mounted at the center of the test section wall. K-type thermocouples are employed to measure temperatures of the molten droplet at the furnace and the water temperature inside the test section. The melt generator consists of induction furnace (260V, 40A) and a graphite cylinder (40mm O.D. x 50mm) with an alumina crucible (20mm I.D. x 30mm) with a 5.0mm hole at the center of the bottom. Molten tin mass of 0.5-0.7g1 is chosen in this series of tests to guarantee the delivery of a single drop into water through the crucible bottom hole. The melt generator, which includes the induction coils and the melt crucible, is housed inside a chamber where argon gas is purged in to

prevent the molten tin from oxidizing during melting. A boron-nitride plug as a melt release plug is used to block the crucible bottom hole during the melting and it is lifted by a pneumatic piston to release the melt drop. The external trigger, located at the bottom of the test chamber, is a piston that generates a sharp pressure pulse similar to a shock wave. The trigger hammer is driven by a rapid discharge of a capacitor bank, consisting of three capacitors that impact on the piston to generate a pressure pulse. The SHARP system as shown in Figure G-1b, consists of a high speed CMOS digital camera (Redlake HG50LE), up to 100000 fps (at present 20000 fps was used) and tungsten lightning for the photography; a continuous X-ray source tube (Philips MCN 321 - max. 320 keV), an X-ray converter, image intensifier and a high speed CCD camera (Redlake MotionScope HR 8000), for the radiographic imaging up to 8000 fps.

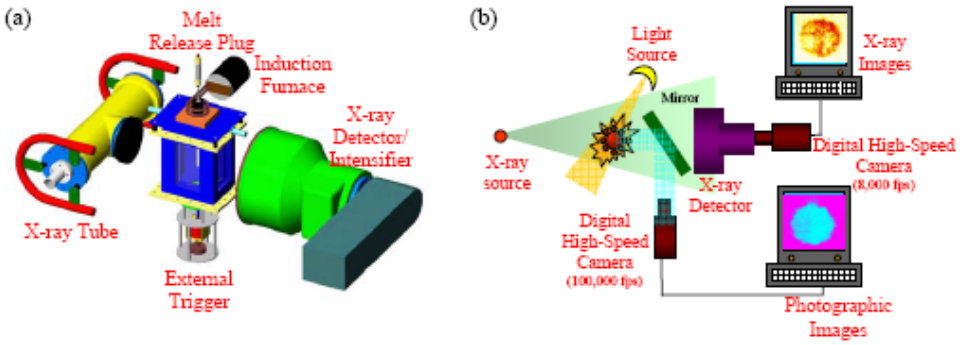

Figure G-1: Schematic diagrams of (a) the MISTEE test facility and (b) the SHARP visualization system.

2.7.3. Simultaneous visualization of vapor bubble and melt fragmentation

The simultaneous X-ray radiographic and photographic images of a 0.56g tin drop at 1000°C in water at 73°C undergoing vapor explosion are shown in Figure G-2. In order to match the images acquired, a series of image processing steps were developed and described elsewhere [7]. The vapor explosion evolution can be depicted into 3 cycles, as indicated on the Figure G-2, which represents an initial expansion and the succeeding collapse of the vapor bubble. t=0 ms is defined as the time when the vapor bubble collapses in the first cycle.

Initially, the undisturbed molten droplet with a diameter of 4.8 mm, undergoing stable film boiling, falls freely into the water with a velocity of 0.6 m/s. At t=-3 ms, the system is disturbed by an externally triggered pressure pulse of 0.15 MPa, as indicated by an arrow in Figure G-2. Liquid-vapor interface instability, induced by the arrival of the pressure wave, leads to the initiation of the first cycle.

During the subsequent bubble growth, -3.25 to -1.25 ms, the molten droplet is deformed although no apparent fine fragments were observed on the vapor interface at this stage. The vapor bubble then reaches its maximum, t=1.25ms, and starts collapsing. The coolant is accelerated towards the deformed droplet, facilitating mixing/direct contact and leading to the 2nd cycle explosive evaporation and fine fragmentation of the droplet. It can be observed that the fine fragments set off in the radial direction following the interface of the growing bubble, t=0.75ms. As the vapor bubble decelerates, the inertia of the fine fragments causes them to go through the bubble surface. The latter reaches its

critical size and the subsequent bubble collapse leaves the fine fragments behind, whereas a fraction of them is redistributed into the center of the initial melt location. At this point, the bubble dynamics can not be precisely discerned since the cloud of fine fragments unable the exact resolution of the bubble interface.

However, the third cycle can be clearly observed, when the collapsing bubble promotes the mixing of the coolant and the remains of the molten material, t=1.50ms, leading to a secondary explosive vaporization. A shell-like region of finely fragmented melt particles is formed just about the water vapor interface during the expansion period, t=1.75 to 2.75ms. The fine fragments are then dispersed within the coolant after the bubble has finally collapsed.

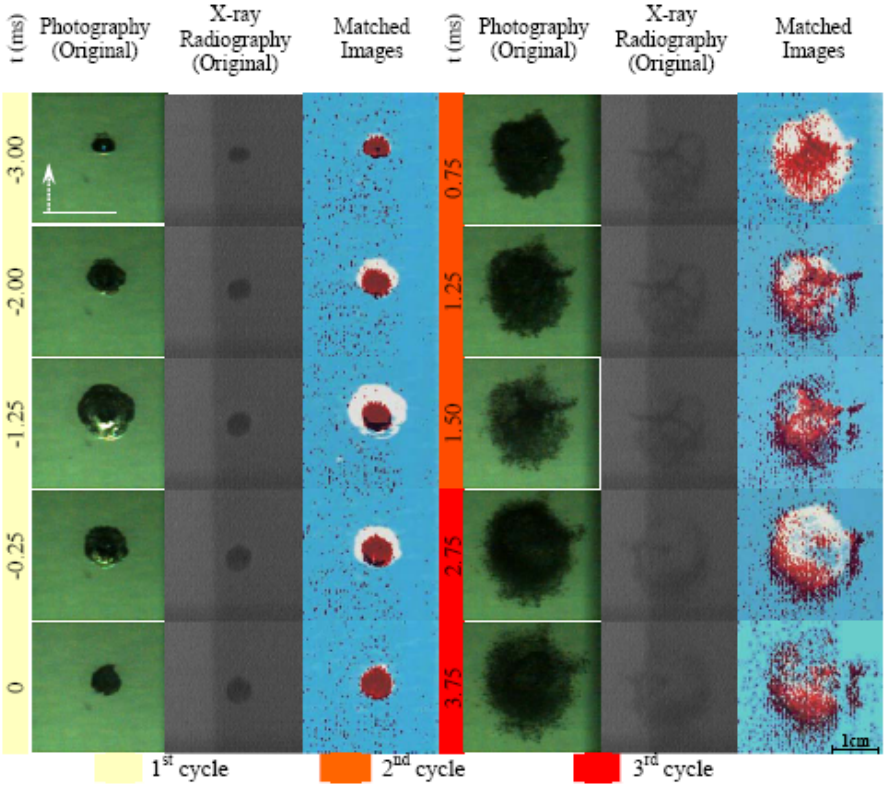

Figure G-2: Synchronized X-ray radiographic and photographic images of a 0.5 g tin drop at 1000°C into water at 73 °C undergoing vapor explosion.

2.7.4. Analysis of bubble and melt dynamics

Bubble Dynamics

The radial growth history of the vapor bubble for different coolant temperatures is represented by the normalized equivalent diameter (D_{eq}) estimated by the image projected area; as shown in Figure G-3, where one can easily identify the 3 cycles mentioned previously: first, -4< t <0 ms; second, 0< t <1.55 ms; third, t >1.55 ms.

The work done by the expanding vapor bubble (W), Figure G-4a, was calculated by estimating the internal pressure using the classical Rayleigh-Plesset equation for bubble dynamics [8]:

$$W(t) = 4\pi\rho_l \int_{R_0}^{R} \left[R^3\ddot{R} + \frac{3}{2}R^2\dot{R}^2 + \frac{2\sigma R}{\rho_l} + 4\mu R\dot{R} \right] dR \tag{G-1}$$

where ρ_l stands for density of the liquid; R for the bubble radius; σ for surface tension; μ for viscosity. Since the energetic interaction is an inertia driven rapid transient, the mass/heat transfer through the interface was neglected [9].

The conversion ratio, CR, shown in Figure G-4b, is acquired then by dividing the work done in Figure G-4a, by the droplet initial internal energy.

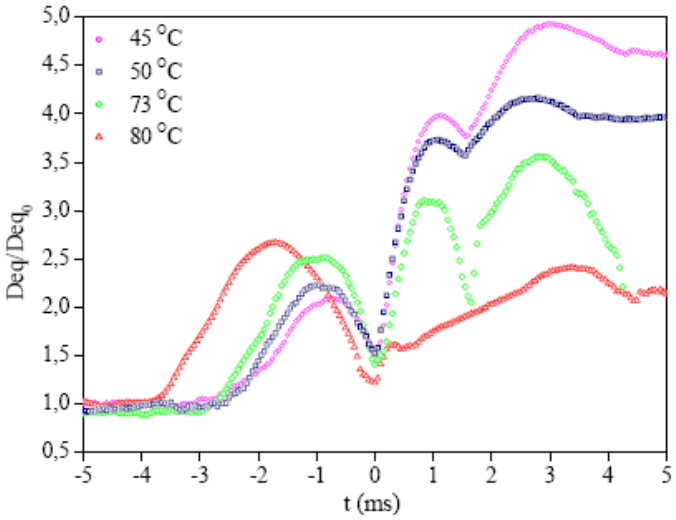

Figure G-3: Radial history for a single tin drop at 1000°C for different water subcoolings.

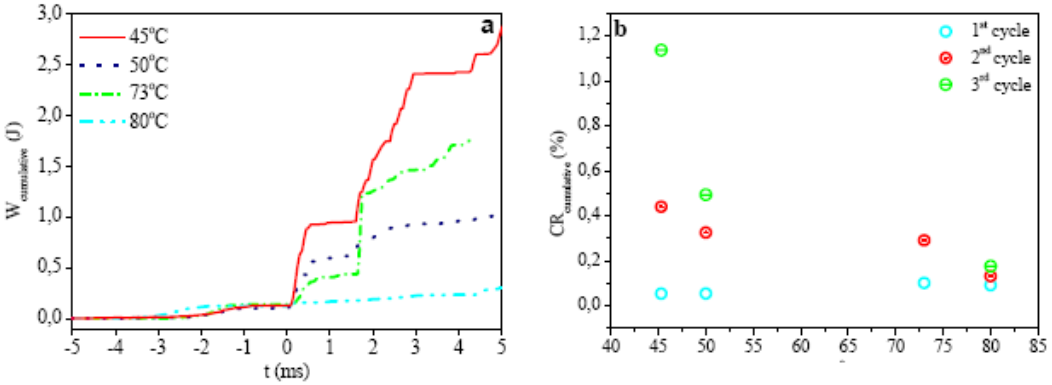

Figure G-4: (a) Cumulative work and (b) Cumulative conversion ratio for different water subcoolings.

Previous works [4,5,6] concluded that higher subcooling should lead to a more energetic steam explosion and this notion is indeed reinforced by the analysis of MISTEE experimental data; Figure G-4a. However, the so-reinforced trend contradicts the perceived picture given by the bubble dynamics during the first cycle: low subccoling would promote a better mixing due to the higher kinetic energy of the collapsing bubble. This finding implies that the bubble dynamics alone can not explain the subcooling effect on vapor explosion.

Melt Dynamics

Since the X-ray radiography gives the projection of the molten droplet, superimposing fragments that are aligned in the X-ray beam direction, a qualitative transient mass distribution, i.e. fragmentation map, can be achieved, granting valuable information on the molten material morphology, which is instructive to the basic understanding of the microinteractions during droplet explosion.

A detailed discussion of the basis and technique for X-ray image processing is given by Hansson et. al. [7] and not repeated here. Insights gained from the MISTEE X-ray results and their comparative analysis with observations and models published by other authors on drop explosion were also given in the above-mentioned paper.

Figure G-5 depicts a typical fragmentation map with a scale from 0 to 100% representing the molten material mass fraction integrated over the incident X-ray beam line. During the vapor bubble collapse, the inrushing coolant promotes the direct contact in the region near the drop surface; Figure G-5c, where the explosive vaporization of the entrained coolant leads to dispersal of the molten material. The fine fragments generated by the microscopically stratified explosion on the melt surface are ejected radially; Figure G-5d, whereas some inner part appears to be compacted by opposite compression forces due to such discrete vapor expansion. Subsequently, during the second bubble collapse, the coolant is accelerated towards the remaining melt, Figure G-5e, where further mixing takes place, leading to the second explosive evaporation, Figure G-5f, and final melt fine fragmentation.

From the X-ray images acquired, one can observe that initial disturbances do not lead to a violent interaction, but render a “slow” vaporization, where the molten droplet experiences deformation/pre-fragmentation; Figure G-5b. Close-up X-ray radiographies of a molten droplet undergoing deformation, Figure G-6, shows the non-homogeneities on the melt surface, Figure G-6b, and density/mass decrease up to 50%, which define the points of coolant entrainment, Figure G-6c, and respective violent evaporation, Figures G-6d and G-6e.

Notably, in his work using a flash X-ray imaging, Ciccarelli [6] observed the formation of fingers and jets on the drop surface already during the first vapor bubble growth and he related this behavior to local high- pressure evaporation at the drop surface. During the bubble collapse, these fingers would be exposed and subject to direct contact with the liquid coolant, leading to the explosive vaporization. Surprisingly, in the MISTEE current setup, similar droplet distortion and melt fingering were not observed. Instead, during the first bubble expansion, the molten droplet is deformed in a more uniform manner, as shown in Figures 5-6b, and no clear structure could be discerned. The swelling of the melt drop is substantial enough to suggest that the droplet experienced interfacial instabilities and disintegration.

It is worth noting that in an early work on droplet explosion, Kim and Corradini [10] proposed that coolant entrainment mechanism is impelled by Rayleigh –Taylor instabilities that follow the vapor film disturbance. This mechanism was later disputed as unlikely, when Inoue et al. [11] showed that the difference of densities was too high to allow for coolant entrainment into the molten material. However, the initial conditions

for the subsequent bubble collapse are established, given that, the later will provide the kinetic energy sufficient to overcome the droplet surface tension.

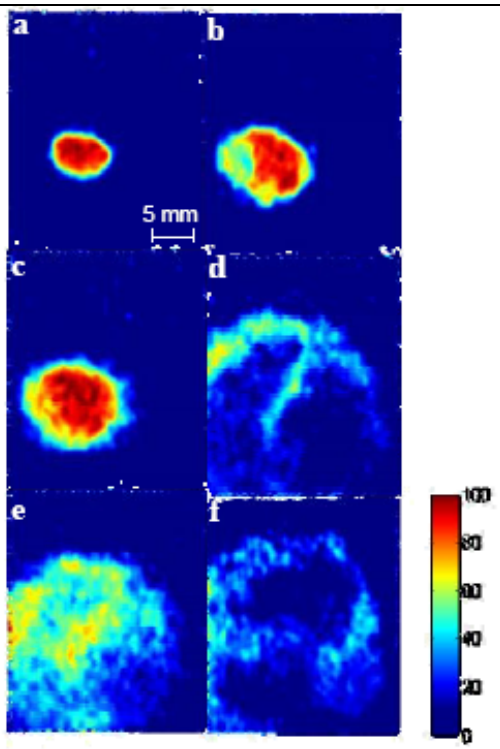

Figure G-5: Quantitative fragmentation map of a 0.5 tin drop at 1000°C into water undergoing vapor explosion at (a) -1.5ms, (b) -0.25ms, (c) 0.125ms, (d)1ms, (e) 1.825ms and (f) 3ms.

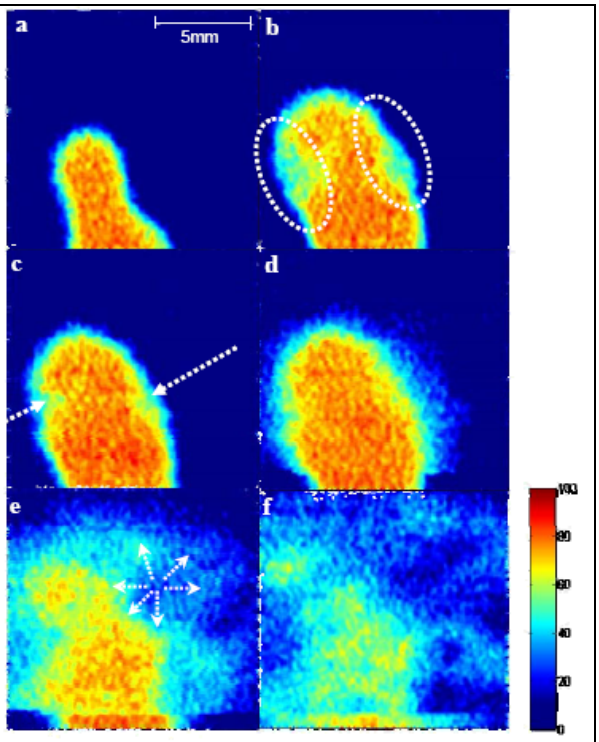

Figure G-6: A partial close-up of a molten droplet qualitative fragmentation map of a typical single drop vapor explosion at (a) -1.5 ms, (b) -0.5ms, (c) 0ms, (d) 0.25ms, (e) 0.5ms and (f) 0.75ms.

2.7.5. Preconditioning for an energetic interaction

Deformation/prefragmentation of a molten drop can be quantified by its average density/thickness and the projected area evolution during the 1st cycle. It can be seen from Figure G-7 that the droplet deformation/prefragmentation decreases with the increase of coolant temperature. This behavior can be explained by the effect of coolant temperature on the stability of vapor film that envelops the molten droplet prior to pressure perturbation. The higher the coolant temperature, the thicker and more stable the vapor film is. Accordingly, when disturbed by an external trigger, pressure oscillations in the vapor-liquid interface would be damped effectively on a thicker film (such as in low-subcooling case) [13,14,15], hence suppressing local coolant-melt contacts and resulting in a more limited deformation/prefragmentation of the molten droplet. Such a compact, non-deformed drop resists liquid coolant entrainment and meltcoolant mixing needed for subsequent explosive expansion.

It is logical to suggest that the greater the melt drop's deformation/prefragmentation the easier it is for the coolant to entrain. That is to say that the pre-fragmented melt drop allows a larger mass of volatile coolant to permeate deeper into the melt interior upon the bubble collapse. The enhanced mixing environment is more favorable to subsequent

explosive vaporization, which reflects on the second bubble dynamics cycle and melt material dispersal, namely the energetics. This hypothesis is confirmed by MISTEE tin-drop explosion data which exhibits a strong correlation between the droplet transverse area ratio (i.e. final-to-initial droplet area during the first cycle) and the second cycle cumulative conversion ratio as shown in Figure G-8.

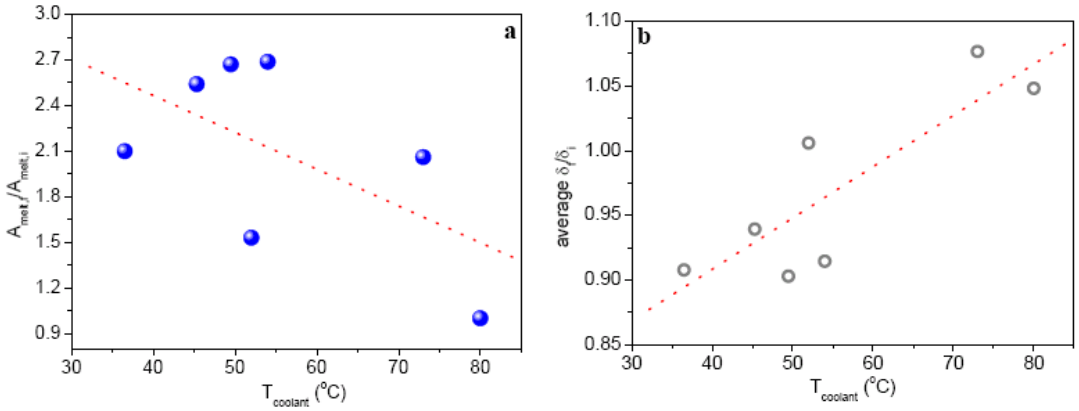

Figure G-7: Molten droplet deformation/prefragmentation represented by the (a) projected area, A_{melt}, and (b) density/thickness, δ, in respect to the coolant temperature

Thus, the MISTEE X-ray data on melt dynamics provides resolution to an apparent controversy about the effect of water subcooling on the first-cycle bubble dynamics vs. explosion energetics discussed in Section 2.7.4. In fact, the MISTEE data shows how the data on bubble dynamics alone could be misleading. Remarkably, most previous models and theories of droplet explosion were derived and validated from images on the bubble dynamics. Simply put, data on evolution of melt material and its relation to bubble dynamics and energetics did not exist prior to the present study. The MISTEE X-ray data of the melt droplet undergoing vapor explosion shown here lead to a discovery of the dominant role of melt dynamics over bubble dynamics in understanding fundamental mechanisms of micro-interactions.

The observations made in MISTEE experiments and the correlation established between the explosion energetics and the droplet deformation provide a basis to suggest that the deformation/prefragmentation of the molten droplet during the first cycle is prerequisite for an energetic vapor explosion in thermal fragmentation regime. We name this mechanism *"**preconditioning**"* of melt droplet for explosion.

Implications of the governing role of melt preconditioning on vapor explosion are broad and far-reaching. For instance, one can arguably relate the oxidic corium's lower explosivity to corium drop being less "preconditioned" to trigger an explosion than a drop of other molten materials used in FCI testing, typically alumina or steel. On the melt-drop side, due to corium's higher temperatures (compared to alumina and steel), the radiation heat flux is more intense, promoting a rapid surface cooling prior to pressure perturbations. Surface of molten metal (e.g. steel) drops remains in the liquid phase for a longer period (than corium) due to the lower temperature level, lower emisivity and significantly higher thermal conductivity which effectively transfers the heat from the droplet interior toward the surface region. Formation of a thin crust or even a mushy layer on the drop surface would significantly increase the viscosity and effective surface tension, rendering the drop resilience to external forcing, including disturbances due to local melt-coolant contacts. In fact, for non-eutectic materials, it suffices to remove only

a fraction of the latent heat of fusion to bring the melt into a mushy state. On the coolant side, the higher radiative heat flux leads to a higher evaporation rate, thicker vapor film and effectively lower subcooling due to energy deposition in water region adjacent to vapor-liquid interface. Correspondingly, a binary non-eutectic oxidic corium melt drop can form a more stable vapor film and a deformationresistant mushy surface layer in a much shorter time than a droplet of molten alumina, steel or even eutectic corium [1].

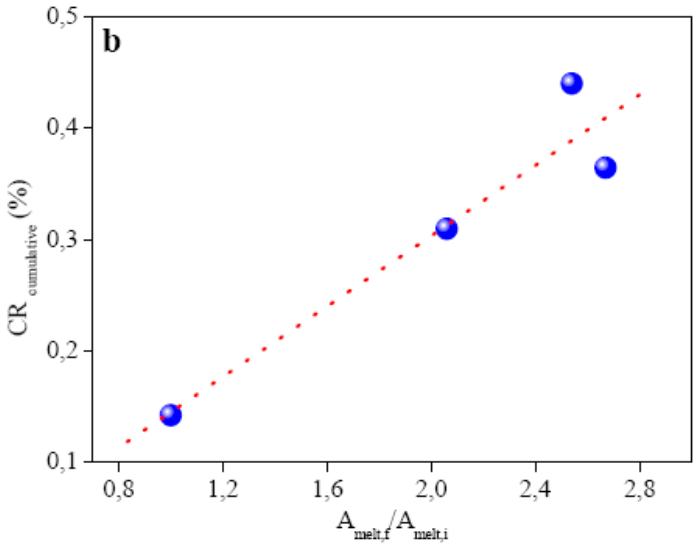

Figure G-8: Second cycle cumulative conversion ratio in respect to molten droplet deformation/pre-fragmentation

2.7.6. Concluding remarks

Single drop vapor explosion experiments were conducted by using the SHARP system which was developed to visualize and characterize the evolution and coupled dynamics of vapor bubble and molten material, granting first-of-a-kind data on micro-interactions in droplet explosion.

The analysis of data obtained in the experiments on vapor bubble dynamics shows that, in low subcooling runs, a favorable initial condition for a more energetic interaction (large kinetic energy of the collapsing bubble, i.e. water hammer) is established during the bubble's 1st cycle – a notion contradicting the results obtained in the bubble's 2nd cycle and the conventional wisdom where lower conversion ratios are expected in low-subcooling cases. Since the bubble dynamics alone does not explain the subcooling effect on vapor explosion energetics, detailed analysis of the melt droplet dynamics becomes crucial. Translated from the X-ray radiography intensity image, the qualitative two-dimensional transient distribution of the fragmented particles and profile history were attained revealing the melt droplet internal dynamics. The obtained images point to *coolant entrainment* into the droplet surface as the mechanism for direct contact/mixing ultimately responsible for energetic interactions. Furthermore, the data exhibits an inverse correlation between the coolant temperature, which characterizes the dynamics of the first cycle in bubble dynamics, and the molten droplet deformation/prefragmentation. The latter named *melt preconditioning* is in turn found to be directly proportional to the vapor explosion conversion ratio. The newly established insight about the role of melt droplet dynamics paves way to speculation that a mechanistic treatment of the droplet

preconditioning can lead to a basic understanding and quantification of how melt physical properties influence steam explosion's triggerability and energetics.

References of Part G

[1] T.N. Dinh, A.T. Dinh, J.A. Green, B.R. Sehgal, "An Assessment of Steam Explosion Potential in Molten-Fuel-Coolant Interaction Experiments", Proc. of the 6th International Conference on Nuclear Engineering, San Diego, USA, May 1998.

[2] M.L. Corradini, B.J. Kim, M.D. Oh, "Vapor Explosions in Light Water Reactors: A Review of Theory and Modeling", *Prog. Nucl. Eng.*, **Vol. 22(1)**, pp.1~117 (1988).

[3] W.W. Yuen, X. Chen, T.G. Theofanous, "On the fundamental microinteractions that support the propagation of steam explosions". Nuclear Engineering and Design, **Vol. 146**, 133–146, 1994.

[4] X. Chen, R. Luo, W.W. Yuen, T.G. Theofanous, "Experimental Simulation of Microinteractions in Large Scale Explosion", *Nucl. Sci. Eng.,* **Vol.189**, pp.163~178, 1999.

[5] L.S. Nelson, and P.M. Duda, "Steam Explosion Experiments with Single Drops of Iron Oxide Melted with a CO2 Laser," *NUREG/CR-2295*, NRC, USA, 1981.

[6] G. Ciccarelli, "Investigation of Vapor Explosions with Single Molten Metal Drops in Water Using Flash X-ray", Ph.D. Thesis, McGill University, Canada, 1991.

[7] R.C. Hansson, H.S. Park, T.N. Dinh, "Simultaneous High Speed Digital Cinematographic and X-ray Radiographic Imaging of a Multi-Fluid Interaction with Rapid Phase Changes", *6th International Conference on Multiphase Flow,* Leipzig, Germany, 2007.

[8] M.S. Plesset, "The Dynamics of Cavitation Bubbles", *ASME J. Phys. Soc.,* **Vol. 64B**, pp.228~231, 1949.

[9] Private communications with Prof. Amir A. Gubaidullin, Tyumen Branch of Institute of Theoretical and Applied Mechanics, SB RAS, Tyumen

[10] J. Kim, M.L. Corradini, "Modeling of Small Scale Single Droplet Fuel/Coolant Interactions", *Nucl. Sci. Eng.*, **Vol. 98**, pp. 16~28, 1988.

[11] Inoue, S. Lee, "Studies on Micro Structures at Vapor Liquid Interfaces of Film Boiling on Hot Liquid", *JAERI Conf 97-011* (Part 1), 1998.

[12] Inoue, A., Aritomi, M., and Takahashi, M., 1992, "An Analytical Model on Vapor Explosion of High Temperature Molten Metal Drop in Water Induced by a Pressure Pulse," Chem. Eng.Comm., Vol. 118, pp. 189~206.

[13] B.J. Kim, M.L. Corradini, "Recent Film Boiling Calculations: Implication on Fuel-Coolant Interactions", *Int. J. Heat Mass Transfer*, **Vol. 29**, No.8, pp.1159~1167, 1986.

[14] B.J. Kim, "Oscillatory Behaviors in Initial Film Boiling: Implications on the Triggerability of Single Droplet Explosions", *KSME Journal,* **Vol. 3**, No.2, pp. 153~158, 1989.

[15] D. Tochio, Y. Abe, "Film Collapse Behavior on High Temperature Particle Surface", *JAERI Conf 99-005,* 2000.

2.8. *Part H:* Material property effect in steam explosion energetics: *Revisited*

2.8.1. Energetic fuel-coolant interactions in LWR severe accidents

Molten fuel-coolant interactions (FCI) have been studied over the past several decades in the context of nuclear reactor safety; see e.g. Corradini et al (1988), Theofanous (1995). The resulting energetic steam explosions in a flooded reactor cavity may challenge the containment integrity. The present study is motivated to pursue the understanding of such an ex-vessel steam explosion, which is of great importance to the severe accident management (SAM) strategy adopted for Swedish boiling water reactors (BWRs), which calls for establishing a deep, subcooled water pool in the lower drywell prior to the RPV failure and release of corium materials from the reactor vessel lower head to ex-vessel space, so as to promote melt fragmentation and coolability on the cavity basemat.

Time-wise, the steam explosion is characterized by three distinctive phases: pre-mixing, triggering and explosion. During the premixing phase, a premixture is formed. Typically, the premixture contains melt drops resulted from the fragmentation of a melt jet. The melt drops, at high temperatures, are surrounded by a vapor film. Explosion occurs by the virtue of liquid-liquid contact, namely molten core material on one side and water on the other side. The yield of an explosion is due to the mechanical energy associated with a multiphase thermal detonation when the pressure wave passes through the pre-mixture. In other words, during a very short time, a fraction of thermal energy stored in the molten materials is liberated in the form of coolant evaporation.

In previous assessments, it was assumed that a large molten pool (ranging from 50 tons to 200 tons of dominantly oxidic corium) already exists in the RPV lower head prior to its failure. This oxidic core melt is then discharged through the RPV failure site, such as a failed vessel penetration (e.g. instrumentation guide tube). Such a perceived picture of the ex-vessel FCI scenario reflects in the problem setup and conditions chosen for the cases studied in the OECD/NEA SERENA project (see Magallon et al, 2006).

It is instructive to note that only the first release of materials from the corium pool in the RPV lower head has the highest potential for energetic steam explosion. After the first release of the molten materials available in the lower head when the vessel fails, the subsequent material release is caused by debris remelting driven by decay heat generation and dripping-off through the RPV failure site. Thus, both the mass discharge rate and the superheat of the melt are limited in the subsequent release phase. For the risk-significant “first release”, both the composition and mass of the corium available for discharge are highly uncertain. It has been argued that it is more likely that after the dryout of debris beds in the lower plenum, melting of structural materials (Zr, steel) commences well before the melting of oxidic (UO_2-ZrO_2) corium due to the metal’s significantly lower melting temperatures (1800K vs. 2800K). In fact, the radiative heat transfer from the heated debris beds may cause the vessel penetrations (metals) to fail long before the formation of an oxidic melt pool in the vessel lower head.

Consequently, one can expect that the first release from a BWR lower head is rich in superheated metallic melt. Such a melt is known to be more explosive in water. At the same time, we expect a limited discharge flowrate due to substantial hydraulic resistance of the (still solid) oxidic debris, through which the metal melt flows toward the RPV

failure site. While a detailed quantification of the melt accumulation in, and discharge from, the RPV lower head and scenario calculations are beyond the scope of the present study, the above discussion already suggests:

(a) a low likelihood of a *large oxidic melt* pool being the first release from a BWR to the ex-vessel water pool, and

(b) a possible scenario with the first release being *superheated metal-rich melt* but limited in discharge flowrate, and hence expectedly being of limited energetic potential.

In the remainder of this study we will focus on the residual-risk situation with predominantly oxidic melt release. In fact, a majority of FCI experiments conducted in the past and planned for the near future employ a range of UO_2-ZrO_2 compositions as representative corium composition. Of relevance and high interest is the TROI program conducted in KAERI (see Song et al, 2006). Most notably, the results of the TROI experiments conducted with different corium composition show a consistent trend of lower conversion ratio (energetics) of non-eutectic corium compared to eutectic corium.

The main questions we ask are:

- (q.1) what are mechanisms that govern the low explosivity in FCI experiments made to date using prototypic corium melts, and
- (q.2) how such an experimental observation applies to reactor predictions. Our attention her is focused on the potential effect of melt material properties.

2.8.2. Corium low explosivity: Revisiting Dinh et al (1998)

Questions about the effect of melt material properties on steam explosion energetics have been imminent and asked repeatedly in the past, largely motivated by stark observations in the KROTOS experiments where the alumina (Al_2O_3) melts exploded spontaneously and energetically whereas the oxidic corium melts (UO_2-ZrO_2) were found resilient to explosion (Huhtiniemi et al., 1999; Huhtiniemi and Magallon, 2002). However, a lack of mechanistic understanding of the underpinning physics did not allow one to explicitly take credits of the potential effect in reactor predictions and risk assessment. In fact, as we look back on the evolution of the views on steam explosion energetics, several distinct periods can be identified with key studies and experimental programs.

1970-1980: period of panic (SL-1, α-mode containment failure, WASH-1400 (1975), thermodynamic model of Board, Hall and Hall (1975), CR of 30-40%)

1980-1990: period of realism (Winfrith, SNL tests, thermite melt, UO_2, single drop tests, CR of 10-20%)

1990-2000: period of (false) optimism (KROTOS, FARO, PREMIX, no explosion)

Opposite trends: [*corium not explosive, i.e. forgetting about early tests*] vs.[*conservative bounding not taking credit for corium low explosivity*]

2000-2007: period of doubt and loss (explosions observed in FARO-33 and TROI, low conversion ratio; SERENA-1 brought scattered simulation results)

After three decades of investigation, the theme of corium low explosivity continues to be at the center of international FCI research, with a hope that years 2010-2015 may be identified as "period of comprehension" when a better understanding and predictability of steam explosion energetics can be achieved. Several prototypic corium experiments are planned in KRTOTOS and TROI within the proposed SERENA-2 program (Magallon, 2007), along with analytical experiments (e.g. MISTEE; Hansson 2007a) and numerical simulations. It remains unclear how the planned experiments and analyses help unravel the long-standing puzzle about the corium low explosivity.

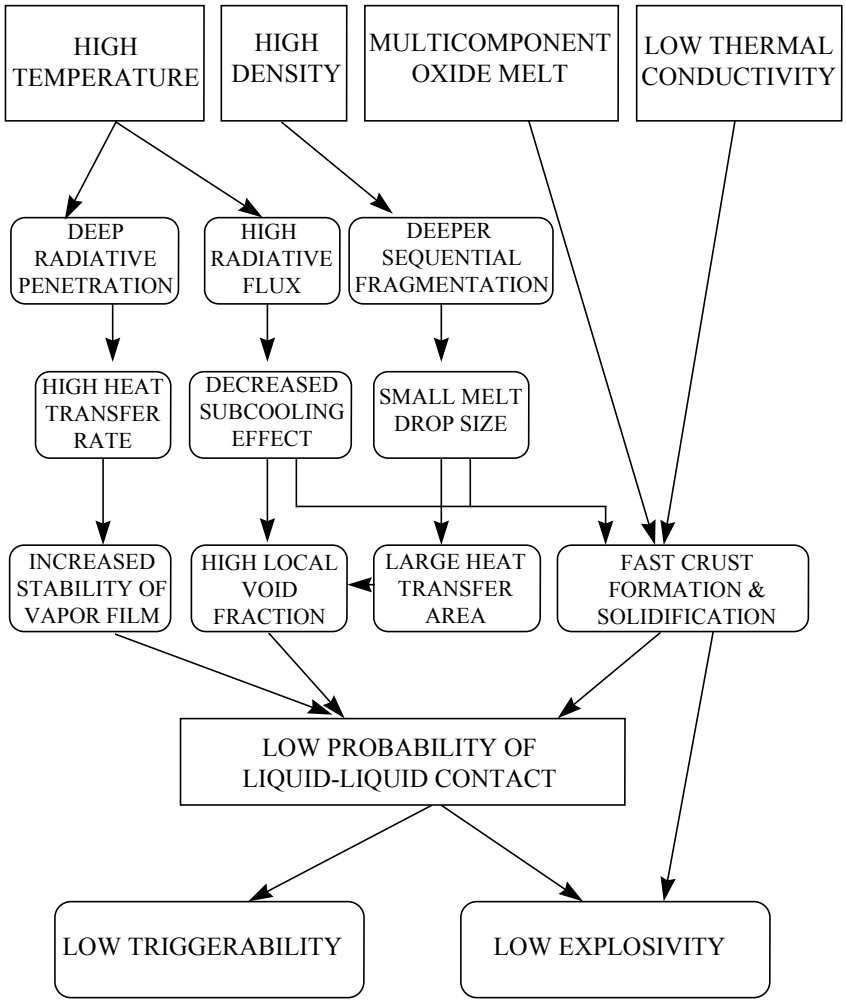

Figure H-1: The role of corium properties in a steam explosion (Dinh et al, 1998).

In a study of Dinh et al (1998), we submitted a view that the low explosivity of corium melt is multi-faceted and yet decomposable and mechanistically explainable; see Figure

H-1. Notably, the 1998 study associated the effect of melt physical properties with the processes in the pre-mixing phase in terms of

(1) corium's higher temperatures (*high void and stable film boiling, rapid cooling*),
(2) corium's higher density (*causing fragmentation to small drops*),
(3) eutectic-*versus*-non-eutectic (mushy) composition (*fast stiff shell formation, solidification*)
(4) oxidic material low conductivity (*surface cooling and crust formation*)

being central to the different explosivity in binary oxidic corium vs alumina melts.

Items #1, 2 and 4 are rather straightforward and consistent with analytical evaluation (for items #1 and 4) and experimental evidences (in KROTOS tests for item #2). The corium's high temperature (item #1) and high emissivity lead to high radiative heat flux which facilitates rapid cooling and solidification. This radiative cooling effect on corium particle solidification, together with small sizes of corium particles (item #2) and low conductivity (item #4) played a central role in the Dinh et al (1998) treatment. The effects can be "measured" by conversion ratio (CR), as shown in Figure H-2. In a recent study, Dombrovski and Dinh (2007) made further qualification of heat transfer in melt particles, reinforcing the notion that the intense radiative cooling during the premixing process limits the explosive potential by reducing the amount of molten materials (in FCI experiments). Noteworthy, the formation of a crust of the same relative thickness occurs much faster in corium than in alumina.

Ideally, the effect of individual properties can be characterized by conducting FCI tests with a well-defined difference in the selected material property while maintaining similarity of all other properties and conditions. However, such an ideal "separation" of the effects is not easily achievable in a FCI testing. Therefore, only a qualitative characterization of the effects is possible through the measured conversion ratio as shown in Figure 2.

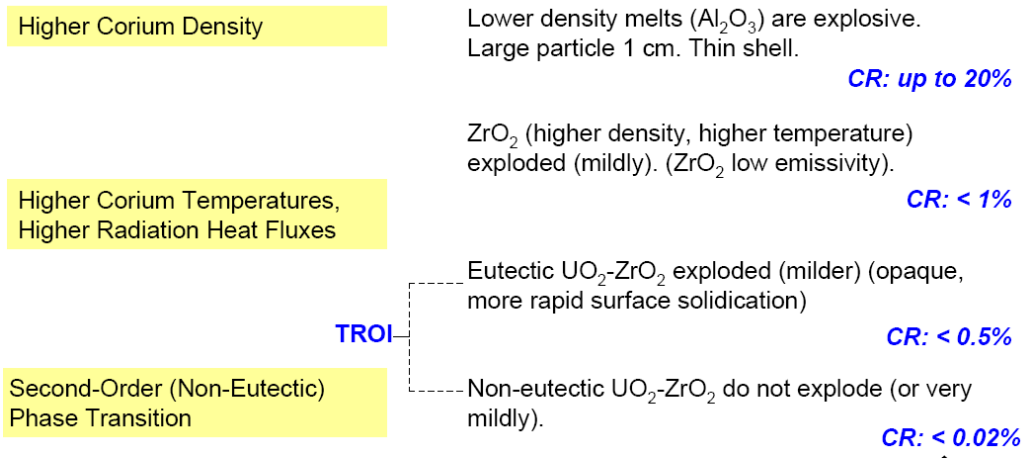

Figure H-2: Conversion ratio (CR) decreases in three steps, indicating the suppression effect of different properties and factors. Note that the conversion ratios are characteristic of small-scale (small-mass) experiments (ALPHA, KROTOS and TROI). Note also that conversion ratios were determined differently in different experiments; CR values also varied in similar tests. Therefore, CR values are taken as maximum measured and shown here to illustrate a trend and order-of-magnitude effect.

Thus, one may rightfully suggest that the CR reduction from 20% to the level of 0.5%...1% (cf. Figure H-2) is associated with pre-mixing, and therefore computable with an appropriate mechanistic treatment of governing processes, namely (i) jet fragmentation, (ii) radiative heat transfer in multiphase (water/steam/melt) media, and (iii) cooling and solidification of the melt particle. In fact, CFD-based computer codes, such as PM-ALPHA.L.3D (Theofanous et al, 1999b) provide the platform for implementation of such models. It is instructive to note that items (ii) and (iii) were treated mechanistically, and item (i) was treated parametrically (using particle size characteristic of the size distribution obtained from FCI tests with a prototypic corium) in the PM-ALPHA.L.3D code. In other words, the predictions of reactor accident scenarios using the PM-ALPHA.L.3D code had already accounted for a major effect of melt properties on the FCI premixing.

Item #3, i.e. the "mushy zone" effect was seen as speculative and met with skepticism by the 1998 paper's reviewers. In fact, at that time, the main FCI database, FARO and KROTOS experiments, included only tests with non-eutectic UO_2-ZrO_2 corium composition. These prototypic corium tests did not produce spontaneous or triggered energetic explosions. However, steam explosions were observed in more recent tests using "eutectic corium" (70-30wt%) UO_2-ZrO_2 melts in the TROI experimental program which employs prototypic materials with both eutectic and non-eutectic corium compositions (Song et al, 2006).

Given all other equivalent pool/jet conditions and melt physical properties, and the "mushy" behavior being the only distinguishing feature between explosive (eutectic, CR max 0.35%) and non-explosive (non-eutectic, CR max 0.02%) melts, the appeal for the hypothesis in item #3 has since increased (Song et al, 2006). Interestingly, scrutinizing the FCI database beyond the TROI experiments, we found that the effect of multi-component melts on steam explosion can be traced back to earlier experiments. Al_2O_3-based multi-component oxidic melt in PREMIX tests and oxide/metal melts (including 25% Zr and 15% Fe) in COTELS tests are found to be more resilient to explosion than the pure alumina in KROTOS tests (CR reported between 0.5% to 5%) or pure metallic Zr in ZREX tests (Cho et al, 1998). Similarly, the FARO binary oxidic melt tests did not explode energetically, whereas the early tests in Winfrith using thermite-generated UO_2 resulted in energetic interactions.

In Dinh et al (1998), we argued that the mushy zone effect is active in the premixing phase and associated with early formation of a surface layer that becomes stiff enough to resist external forces. The results of radiative/conductive/phase-change calculations performed for oxidic corium particles suggest that the width of the mushy zone (between the solidus and liquidus) is small. As such, it has little effect on solidification behavior of the melt particle. Furthermore, the time window for the mushy zone to exist on the particle surface is small compared to the premixing time. Consequently, the experimentally-observed *effect of the melt's non-eutectic composition should be sought in fine fragmentation* during the explosion phase. *This notion of the "mushy" effect on micro-interactions presents a major deviation from the previous study (Dinh et al, 1998)* that suggested the role of the "mushy" zone in solidification during the FCI premixing.

2.8.3. Material property effect on micro-interactions

Micro-interactions that govern energetics

In the present study, the following conceptual picture of micro-interaction is considered. Upon the passage of a pressure wave, the vapor film around the melt droplet is collapsed to allow liquid-liquid (melt/coolant) contact. Instantaneous contact with hot melt causes the water to heat up, forming a layer of width δ_W beyond homogeneous nucleation temperature T_{HN}. The δ_W-layer will evaporate explosively, forming a growing bubble around the melt drop. Another concurrent, always active mechanism for heat transfer is radiation from the melt surface. However, during the micro-interactions radiation heat transfer plays an increasing role: due to hydrodynamic interactions with coolant, the melt drop surface experiences instabilities, significantly enlarging the surface areas for radiation heat transfer. Such radiative heat transfer evolves with the interfacial area evolution that depends on breakup regime and has a characteristic time of drop breakup t_{BR} (T_{BR}). A fraction of the radiative heat flux is absorbed in a subcooled water pool, while the rest causes evaporation at the bubble wall or any liquid coolant within the micro-interaction zone. The interaction scheme is illustrated on Figure H-3.

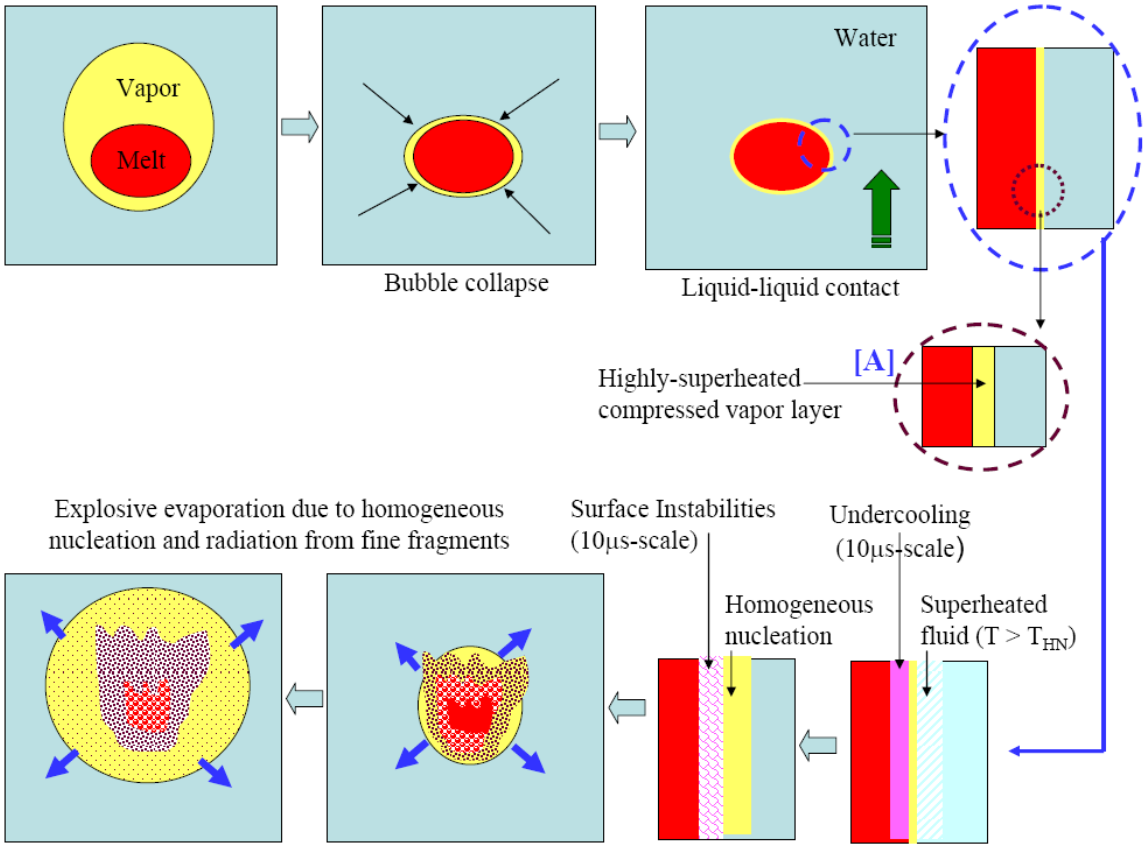

Figure H-3: Mechanisms active in micro-interactions that followed a shock wave passage. Evaporation rate is governed by homogeneous nucleation of superheated fluid and by radiative flux from the fine-fragment cloud formed due to catastrophic breakup of the drop. (melt drop in read; vapor bubble in yellow).

Thus, the present study associates micro-interactions with degree of fine fragmentation (and subsequent radiative flux), whereas previous considerations placed their focus on entrainment of liquid into the micro-interaction zone (and subsequent evaporation). Even though the two processes of melt fragmentation and liquid entrainment are tightly coupled in micro-interactions, the shift of focus from entrainment to fragmentation is central to our ability to relate the explosion efficiency to melt physical properties associated with fine fragmentation.

Within the above-described physical picture, the following remarks can be made.

(i). If the premixing zone is highly voided, the pressure wave would cause collapse of vapor film around melt drop as well as other bubbles in the vicinity. Such a collective collapse would effectively reduce velocity of the coolant impact onto melt drop. Such behavior is consistent with observations that voided pre-mixtures are less explosive.

(ii) As the coolant interfaces approach and contact the melt drop interface, a contact temperature, T_{IN} , established is that in-between the melt temperature and the coolant temperature. Given an ideal, instantaneous contact, a solution for two semi-infinite bodies applies

$$\frac{T_M - T_{IN}}{T_{IN} - T_W} = \sqrt{\frac{(kC_p\rho)_W}{(kC_p\rho)_M}} = \xi \quad \text{or} \quad T_{IN} = \frac{T_M + \xi T_W}{1+\xi} \tag{3}$$

The lower the thermal conductivity of the melt, the lower T_{IN} . Such trend is consistent with observations of the high explosivity of high-superheat and metallic melts, since the surface upon contact remains unconditionally liquid, permitting interfacial instabilities and subsequent breakups.

In the prototypic reactor accident scenario, however, the ideal contact is not realized. Furthermore, due to the high temperature of corium melt, the vapor sublayer adjacent to the melt drop is highly superheated (Dinh et al, 1999). Consequently, even in the wake of a shock wave, the local vapor enthalpy remains higher than saturation enthalpy for local pressure, leaving a thin, compressed layer of vapor between the melt drop and the collapsing bubble wall; see insert [A] of Figure H-3. Accurate solutions for the contact heat transfer problem must therefore consider the vapor layer resistance, which will reduce T_{IN} .

(iii) If the surface temperature, T_{IN} , is sufficiently low, the contact leads to formation of a layer of width δ_M with the temperature lower than the drop's melting point T_{MP}, causing a rapid crystallization in the δ_M layer. Given no interfacial instabilities and breakups, the evaporation is limited to homogeneous nucleation in δ_W-layer and radiation heat transfer from the drop's original (but now cooled to T_{IN}) surface. Such a limited evaporation would not suffice to create an explosion and sustain a detonation wave.

(iv) Following the liquid-liquid contact, the melt surface becomes undercooled, well below its freezing point. Thermodynamically, the undercooled melts are metastable, creating conditions for nucleation and formation of various metastable

solids. It is well known from the literature on phase changes that nucleation can be homogeneous and heterogeneous. The presence of impurities in the melts largely reduces the nucleation energy barrier and facilitates heterogeneous nucleation. There exists an activation threshold for crystallization with origin in the activation energy (or nucleation energy barrier) required to form a critically sized nucleus that can lower its energy by growing further. In other words, the maximum undercooling achievable for a melt is associated with nucleation phenomena in a metastable state. The undercooling thus creates a force due to the Gibbs free energy difference that drives crystallization. This force increases with undercooling.

Phenomena that govern fine fragmentation

The above remarks lead us to suggest that steam explosion energetics being driven by fine fragmentation is governed by three rate processes: surface undercooling, recalescence (nucleation and growth of solid phase with release of latent heat), and interfacial instability and breakup. Time-wise, it can be seen from the estimates (10-100 μs) given in this section that these processes are competitive.

(a) Surface undercooling of melt drop upon contact with water

Upon the contact with coolant, the cooling rate (dT/dt) of melt drop surface can reach to 10^8K/s, i.e. 1000K over a short period t_{SC} ~10μs. Over such a short time scale, a thermal boundary layer of $\delta_M = \sqrt{\alpha_M . t}$ = 1..10 μm can develop on the drop surface.

The undercooling is, however, resisted by crystallization. It has been established that nucleation undercoolings ΔT_N increase linearly with cooling rate, i.e. $\Delta T_N \sim (dT/dt)$. For different materials, the hypercooling limit is 200-500K, although measured nucleation undercoolings were smaller, e.g. 100-200K. For binary mixtures, large undercoolings were reported for containerless eutectics, both oxides and metals (Li et al., 2004). However, for micro-interactions, the melt drop surface is in contact with water, providing abundance of sites for nucleation. The undercooling is therefore limited as illustrated in Figure H-4.

(b) Nucleation and dendrite growth under a highly non-equilibrium condition

It is known for non-equilibrium solidification as a nucleation-driven phenomenon that given melt composition, the higher the cooling rate, the deeper the undercooling. Computer simulations of non-isothermal solidification of binary alloys such as those performed by Grujivic et al (2002) show that for the solidification (nucleation onset), the delay time is rather independent of the cooling rate and the undercooling itself. However, the characteristic time of solid phase growth t_N is predicted to be proportional to the undercooling and therefore cooling rate. Generally speaking, under high undercooling, nucleation in binary materials becomes extremely complex non-equilibrium process, and it has been studied due to its importance for the material science. In addition, it is known for metal alloys that if the initial melt undercooling (ΔT) passes through the extended liquidus line, eutectic phase is prone to become metastable (e.g. Herlach et al, 2004). The noted "singularity" of eutectic crystallization has inspired us to the present effort.

The driving hypothesis for the effect of melt composition on micro-interactions is that during solidification of the undercooled binary melt occurs earlier and propagates faster in non-eutectic melts than in eutectic ones. The basis and rationale for the above hypothesis can be seen from Figure H-4 for non-equilibrium solidification, in combination with equilibrium phase diagram.

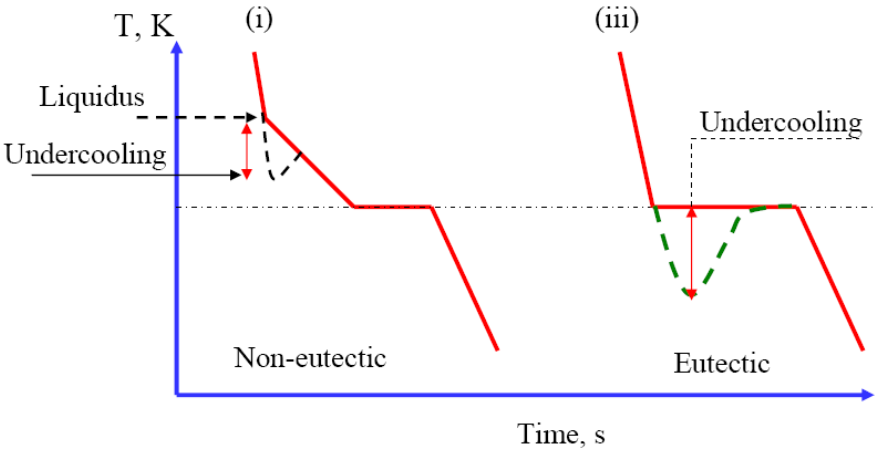

Figure H-4: Schematic illustration of undercooling driven by rapid cooling (e.g. on the drop surface) for two melt composition shown in Figure 3. Deeper undercooling expected to occur in the eutectic case means that in such cases, the drop surface remains liquid for a longer time period, allowing for interfacial instabilities to evolve significantly. In the noneutectic case, the recalescence sets in earlier, rendering the liquid mushy and viscous at a much early time in the solidification transient.

Thermodynamically, one expects the eutectic composition be more stable under unstable undercooled conditions than non-eutectic ones. For the latter, the difference in free energies favors formation of a solid phase, whose (particle-like) microstructures then serve as internal heterogeneities (nucleation sites) to activate the eutectic crystallization. Similarly, the presence of multiple components in a melt introduces microscopic heterogeneity, further strengthening a notion of heterogeneous nucleation under a lowered nucleation undercoolings (nucleation energy barrier). While the conceptual picture of the effect of mushy zone solidification is illustrated in Figure H-4, no data can be found to evaluate the limit of hypercooling ΔT for noneutectic materials, particularly corium or other binary oxidic refractory materials. Molecular dynamics and phase-field simulations are promising tools to obtain important insights and qualification of time scales of the solidification process.

(c) Interfacial instability and fine fragmentation due to coolant impact on drop

The melt drop is subject to a high Weber number condition upon the passage of the shock wave. With the aftershock velocity evaluated as $U_\infty = U_C.\alpha_V$, we have $We = \dfrac{\rho_W U_\infty^2 D_M}{\sigma}$ in the range $10^4 \ldots 10^5$, for which a drop is expected to experience

a Raleigh-Taylor instability and catastrophic breakup (Theofanous et al., 2004). The breakup time can be evaluated as $T_{BR} \equiv \frac{t_{BR}U_\infty}{D_M}\sqrt{\frac{\rho_W}{\rho_M}} = C.We^{-1/4}$, with C= 10-20; or t_{BR} = 100…250μs. The resulting debris size D_F in such catastrophic breakup can be evaluated by using $We_C \sim 10$, i.e. $D_F \sim 10^{-3}D_M$ = 3-5μm. It should be noted that in difference to drop breakup in an ambient fluid (liquid), the coolant surrounding the melt drop evaporates rapidly, creating room for the interfacial instability to growth freely, and for fragments to fly off easily toward the bubble wall region. Clearly, such an expanding cloud of fine-size debris provides an intense source for heat radiation, even when self-attenuation is considered.

Compared to the surface area of the original drop $A_O=\pi\ D_M^2$, the total emitting surface area A of the particle cloud, taken at η=10-100 particles layer, $A = 4(D_M/D_F)^2\ \eta.\pi\ D_F^2$= (40…400) A_O. In fact, while η increases in time during the cloud expansion, the melt surface temperature on small particle decreases in time. One can expect an increase in the effective radiation flux as much as 30-100 times that of the radiation flux from the original drop (q_o~5 MW/m^2).

Melt viscosity is also known to contribute to the breakup. When melt viscosity is larger than a threshold, it causes increase of both breakup time and fragment size. During the cooling and growth of dendritic particles in a mushy fluid, the fluid viscosity increases as the drop surface evolves. While details of such behavior can only be captured and delineated in a direct numerical simulation, it is clear that the breakup time t_{BR} (O~100μs) is long enough for the surface cooling t_{SC} (O~10μs) and crystallization process t_N (O~10μs) to occur and suppress the instability development.

If solidification (a)-(b) prevails over instability (c), the drop surface forms a solid crust or a stiff, highly-viscous mushy layer, suppressing evolution of short-wavelength instabilities. Consequently, hydrodynamic interactions lead only to coarse fragmentation, creating large fragments with a relatively lower surface-to-volume ratio, and correspondingly lower radiative heat flux. If the interfacial instability prevails, a large interfacial area is generated for radiative heat transfer.

The above description provides avenues by which various physical properties of melt influence the competing processes that ultimately govern fine fragmentation. Optical (radiation) properties (emissivity, opaqueness) and conductivity enter item (a) of surface undercooling. Surface tension and viscosity over a range of temperature enter item (c) of interfacial instability. Of relevance to the discussion of the effect of eutectic versus non-eutectic compositions are more subtle thermodynamic properties, which determine conditions and dynamics of nucleation and dendritic growth. This aspect needs further investigation, by well-characterized experiments and numerical simulations using molecular dynamics and phase-field models.

2.8.4. Triggerability versus energetics

The preceding discussion focused on hydrodynamic fragmentation expected to dominate the explosion phase when a strong shock wave escalates and propagates through the premixture. During the explosion's triggering and early escalation, melt drops are subject

to a weak pressure wave (trigger), leading to a collapse of vapor film around the melt drop, and subsequent bubble cycles; see Hanson et al. (2007a) for new visualization of drop explosion in this regime (dubbed thermal fragmentation). It is possible that hydrodynamic interactions can cause vapor film collapse locally, leading to a bubble dynamics as in the case of triggered interaction. Energetic coolant/melt interaction is then observed to occur at the end of the first bubble cycle.

The physics and the effect of melt properties discussed for hydrodynamic fragmentation generally apply to thermal fragmentation as well. Undercooling of the melt drop surface and subsequent rapid formation of the mushy layer govern the low explosivity of non-eutectic oxidic melts. The main difference between the hydrodynamic and thermal fragmentation regimes lies in time scale: in the thermal fragmentation case, the first bubble cycle (couple ms) is available for dendrite growth if the melt is undercooled. Due to such long duration, binary oxidic melts, including both high-temperature corium and medium-temperature stimulant materials, have been observed to be highly resilient against spontaneous or (weak) triggered explosion.

In general, a premixture of low explosivity (combining coolant and melt conditions, and melt properties) is closely correlated with its low triggerability. The opposite may however not hold. A strong trigger can overcome the low triggerability in thermal fragmentation mode. Strong trigger can occur in some prototypic reactor scenarios. For example, if a water pool depth is shorter than the melt jet breakup length, molten materials may spread on the cavity floor, trapping a sizable amount of water under the melt layer. Rapid evaporation of the entrapped water can lead to an energetic trigger for the upper premixture. Such a situation pertains to in-vessel FCIs but not characteristic of ex-vessel FCIs of interest, which involves a deep, subcooled water pool present in the drywell cavity.

2.8.5. Concluding remarks

After a decade since an intensive phase of FCI research ended in the late 1990s (with resolution of safety issues related to containment α-mode failure and vessel lower head failure due to in-vessel steam explosion in a PWR), international efforts have continued in the both experimental and analytical (code) fronts, without substantial advances in further understanding and reducing uncertainties in describing the complex phenomena involved in FCI pre-mixing, triggering and explosion phases. From a risk perspective, there is a need for a robust assessment of ex-vessel steam explosions as a threat on containment integrity in certain LWR plant designs. Given the existing phenomenological uncertainties, reducing uncertainties associated with parameters of the melt's first-release appears a "cost effective" avenue in quantification of ex-vessel steam explosions. In fact, the melt first-release parameters (being boundary conditions to FCI) are highly sensitive to accident progression in the vessel lower head, including (i) vessel failure modes and timing, (ii) amount, composition and superheat of molten materials available for discharge to ex-vessel space, and (iii) vessel hole ablation and relocation path of melt to water pool in a reactor cavity. These aspects are beyond the scope of the present study, but it suffices to say that they are important elements of an integrated assessment underway at KTH (Dinh et al., 2007a).

Returning to the two questions (q.1 and q.2) posed in Section 1, the following can be highlighted. For a given set of FCI initial conditions (pool depth, water temperature,

etc.) and boundary conditions (melt superheat, jet diameter, etc.), there are complex processes of macro-interactions (during premixing) and micro-interactions (during explosion) by which melt material properties govern steam explosion energetics. Most importantly, solidification (on the melt side) and boiling (on the water side) serve to limit the efficacy of subsequent direct liquid-liquid contact. Low conversion ratios measured in small-scale corium experiments (few kg of corium, trigger after melt release completed) are indicative of corium higher resilience to explosion, which however should perhaps be interpreted first as evidence of low triggerability rather than low energetics. Furthermore, due to multiple time scales present in premixing (melt supply duration, particle solidification, trigger time), extrapolation of the measured behavior to reactor situations (involving continuous delivery of many tons of molten corium) is not straightforward.

For the premixing phase, the limiting effect of corium melt properties can already be captured by using the computational platform provided by advanced CFD-based multiphase codes such as PM-ALPHA.L. It is essential that appropriate models are included for the calculation of (a) particle size distribution resulting from jet fragmentation, (b) radiative heat transfer accounting for water/steam/melt's phase distribution and optical properties, (c) spatio-temporal description of radiative/conductive/phase-change (solidification) heat transfer in melt particle. Development and validation of effective treatment of these three processes and their implementation in premixing codes have been pursued under the ongoing MSWI Project (Dinh et al., 2007b).

For the explosion phase, the present study suggests that limiting mechanisms effective in macro-interactions/pre-mixing are also active in micro-interactions. Moreover, experiments on micro-interactions can be made "full-scale" since its configuration deals with a single melt drop with coolant. Data on micro-interactions are very limited highlighting the significance of future experiments on "micro-interactions" over a broad range of materials, including prototypic corium melts. Such experiments may employ a SIGMA shock-tube setting (Chen et al 1999) for simulating realistic explosion conditions and MISTEE/SHARP (Hanson et al., 2007a, 2007b) technique for high-resolution visualization.

Notably, in this study, we propose nucleation-driven solidification behavior upon rapid undercooling of melt drop surface due to liquid-liquid contact being responsible for the efficacy of fine fragmentation, and ultimately steam explosion triggerability and energetics. Further steps to qualify the present hypothesis require combination of well-characterized experiments and molecular dynamics/phase-field simulations to determine the nucleation energy barrier and dendritic growth patterns in binary oxidic (corium) melts, both eutectic and non-eutectic compositions.

References of Part H

Berman, M., "Light Water Reactor Safety Research Program Quartely and Semi-annual Report", Sandia National Laboratories Report, SAND84-2500, 1984. Also NUREG/CR-4459, 1986.

Berthoud, G., "Vapour explosions", *Annual Review of Fluid Mech.* 32 (2000), pp. 573–611.

Bird, M. J. and Millington, R. A., "Fuel Coolant Interaction Stuides with Water and Thermite-Generated Molten Uranium Dioxide", *4th CSNI Spec. Mtg. on FCI in Nuclear Reactor Safety*, Bournemouth, UK, 1979.

Bird, M. J., "An Experimental Study of Scaling in Core Melt/Water Interaction*", 22nd National Heat Transfer Conference*, Niagara Falls, 1984.

Board, S.J., Hall, R.W. and Hall, R.S., "Detonation of Fuel Coolant Explosions", *Nature*, 254 1975;

Buxton, L.D. and Benedic, W.B., "Steam Explosion Efficiency Studies," NUREG/CR-0947, Nov. 1979.

Chen, X., Luo, R., Yuen, W.W. and Theofanous, T.G., "Experimental Simulation of Microinteractions in Large Scale Explosion", *Nucl. Sci. Eng.,* Vol.189, pp.163~178, 1999.

Cho, D.H., Armstrong, D.R. and Gunther, W.H., "Experiments on interactions between zirconium-containing melt and water", NUREG/ CR-5372 (1998).

Corradini, M.L., Kim, B.J. and Oh, M.D., "Vapor Explosions in Light Water Reactors: A Review of Theory and Modeling" *Prog. Nucl. Eng.*, Vol. 22(1), pp.1~117 (1988).

Dinh, T.N., Dinh A.T., Green, J.A. and Sehgal, B.R., "An Assessment of Steam Explosion Potential in Molten-Fuel-Coolant Interaction Experiments", CD-ROM Proceedings International Conference on Nuclear Engineering, ICONE-6, San Diego, USA, May 1998.

Dinh, T.N., Dinh, A.T., Nourgaliev, R.R. and Sehgal, B.R., "Investigation of Film Boiling Thermal Hydraulics under FCI Conditions: Results of Analysis and a Numerical Study"*, International Journal of Nuclear Engineering and Design*, 189, pp. 251-272, 1999.

Dinh, T.N., Ma, W.M., Karbojian, A. Hansson, R.C., Kudinov, P., Park, H.S. et al., "Proceedings of the 23-th Meeting for the APRI/HSK/NKS/SARNET Project on Melt-Structure-Water Interactions", Royal Institute of Technology, 156p. November 15, 2006.

Dinh, T.N., Ma, W.M., Karbojian, A., Hansson, R.C., Kudinov, P., Tran, C.T. et al., "Proceedings of the 24-th Meeting for the APRI/HSK/NKS/SARNET Project on Melt-Structure-Water Interactions", Royal Institute of Technology, 199p. June 20, 2007.

Dombrovski, L. and Dinh, T.N., "The Effect of Thermal Radiation on the Solidification Dynamics of Metal Oxide Melt Droplets", *Nuclear Eng. & Design, 2007*.(submitted)

Grujicic, M., Gao, G., and Miller, R.S., "Computer Modeling of the Evolution of Dendrite Microstructure in Binary Alloys During Non-isothermal Solidification", J*ournal of Materials Synthesis and Processing*, Vol. 10, No. 4, pp.191-203, July 2002.

Elder, K. R., Gunton, J. D. and Grant, M., "Nonisothermal eutectic crystallization", *Physical Review E* Vol 54 (6) Dec 1996

Hansson, R.C., Park, H.S. Dinh, T.N. (2007a), "Simultaneous High Speed Digital Cinematographic and X-ray Radiographic Imaging of a Multi-Fluid Interaction

with Rapid Phase Changes", *6th International Conference on Multiphase Flow,* Leipzig, Germany, 2007.

Hansson, R.C., Park, H.S. and Dinh, T.N. (2007b), "Dynamics and Pre-conditioning of a single drop vapor explosion", The 12th International Topical Meeting on Nuclear Reactor Thermal Hydraulics (NURETH-12) , Pittsburgh, Pennsylvania, U.S.A. September 30-October 4, 2007.

Herlach, D.M., Gao, J. Holland-Moritz, D. and Volkmann, T., "Nucleation and phase-selection in undercooled melts", *Mater. Sci. Eng. A* 375–377, p. 9-15, July 2004.

Huhtiniemi, I. and Magallon, D., "Insight into steam explosions with corium melts in KROTOS", *Nuclear Engineering and Design*. 204, 391-400, 2002.

Huhtiniemi, I., Magallon, D., Hohmann, H., "Results of recent KROTOS FCI tests: alumina versus corium melts", *Nuclear Engineering and Design*, Vol.189, p.379–389, 1999

Kaiser, A., "Melt Water Interaction Tests (PREMIX Tests PM10 and PM11)", *Proceedings of the OECD/CSNI Specialist Meeting on Fuel Coolant Interactions*, Tokai-Mura, Japan, May 1997.

Li, M., Nagashio, K. and Kuribayashi, K., "Containerless solidification of undercooled oxide and metallic eutectic melts", *Mater. Sci. Eng. A*, Vol. 375-377, pp. 528-533, July 2004.

Magallon, D., "OECD/NEA SERENA program" 2006. Also Magallon, D. et al, FCI phenomena uncertainties impacting predictability of dynamic loading of reactor structures (SERENA programme), Workshop on Evaluation of Uncertainties in Relation to Severe Accidents and Level 2 Probabilistic Safety Analysis, Aix-en-Provence, France, November 2005.

Magallon, D., "FCI Research and SERENA-2 Program", Presentation to MSWI-24 Meeting, Stockholm, June 2007.

Marshall, B.W., Beck, D.F. and Berman, M. "Mixing of Isothermal and Boiling Molten-Core Jets with Water: The Initial Conditions for Energetic FCIs," Proceedings of International ENS/ANS Conference on Thermal Reactor Safety, Avignon, France, pp. 117, 1988.

Pilch, M. and Erdman, C.A., "Use of Breakup Time Data and Velocity History Data to Predict the Maximum Size of Stable Fragments for Acceleration-Induced Breakup of a Liquid Drop", *International Journal of Multiphase Flow*, Vol. 13, No. 6, pp 741-757, 1987.

SERG-2, 1995. "A reassessment of the potential for an Alpha-Mode containment failure and a review of the current understanding of broader fuel-coolant interaction (FCI) issues. NUREG-1529.

Song, J.H. et al., "Fuel coolant interaction experiments in TROI using a UO_2/ZrO_2 mixture. *Nuclear Engineering and Design,* Vol.222, p.1–15, 2003.

Song, J.H. et al., "The effect of corium composition and interaction vessel geometry on the prototypic steam explosion", *Annals of Nuclear Energy,* Vol.33, 1437–1451, 2006.

Theofanous, T.G., "The study of steam explosions in nuclear systems**",** *Nuclear Engineering and Design*. Vol.155, pp.1-26(26), 1995.

Theofanous, T.G., Yuen, W.W., Angelini, S., Sienicki, J.J., Freeman, K., Chen, X. and Salmassi, T. (1999a) "Lower Head Integrity Under Steam Explosion Loads," *Nuclear Engineering & Design*, 189 (1999) 7-57. Also T.G. Theofanous, W.W. Yuen, S. Angelini, J.J. Sienicki, K. Freeman, X. Chen and T. Salmassi, "Lower Head Integrity Under In-Vessel Steam Explosion Loads,"DOE/ID-10541, 1998.

Theofanous, T.G., Yuen, W.W., and Angelini, S. (1999b), "The Verification Basis of the PM-ALPHA Code," *Nuclear Engineering & Design*, 189 (1999) 59-102. Also T.G. Theofanous, W.W. Yuen and S. Angelini, "Premixing of Steam Explosions: PM-ALPHA Verification Studies," DOE/ID-10504, June 1998.

Theofanous, T.G., Li, G.J. and Dinh, T.N., "Aerobreakup in Rarefied Supersonic Flows", *ASME Journal of Fluids Engineering*. 126 (4), pp.516-527. 2004.

WASH-1400, 1975. U.S. Nuclear Regulatory Commission,1975, Reactor safety study, An assessment of accident risks in U.S. commercial nuclear power plants, USAEC Report, WASH-1400.

Yamano, N., Murayama, Y., Kudo, T., Hidaka, A. and Sugimoto, J., "Phenomenological Studies on Melt-Coolant Interactions in the ALPHA Program", *Nuclear Engineering and Design*, Vol. 155, pp. 369-389, 1995.

Yuen, W.W., Chen, X. and Theofanous, T.G., "On the fundamental microinteractions that support the propagation of steam explosions", *Nuclear Engineering and Design*, Vol.46, p.133–146, 1994.

3. Summary and Perspectives

Under the joint support of the APRI, HSK, SARNET and NKS, significant progress was made and important findings were obtained in the MSWI (Melt-Structure-Water-Interactions) project during 2006-2007. Methodologically, our risk-oriented approach enabled us to identify risk-significant (sub-)phenomena/effects and suggest appropriate level of treatment. Additionally, important new capabilities to perform analyses of these phenomena, at different levels of details, have emerged.

Substantial advances in process modeling and new insights into related mechanisms were gained from the study of corium pool heat transfer in the BWR lower head; debris bed formation; thermal hydraulics and coolability in bottom-fed and heterogeneous debris beds; micro-interactions of steam explosion and the material property effect in steam explosion. Specifically, for analysis of heat transfer in a BWR lower plenum an advanced three-dimensional simulation tool was developed and validated, using a so-called effective convectivity approach and Fluent code platform. The results of scoping experiments and analyses in the DEFOR program strongly suggest that porous beds formed ex-vessel from a fragmented high-temperature debris is far from homogeneous. Both high porosity and heterogeneity are central to the bed's enhanced dryout heat flux and therefore improved coolability. A comprehensive framework was introduced and advanced diagnostic and image processing techniques are examined to enable quantitative analysis of complex multi-phase processes that govern debris bed formation. Results of calculation of bed thermal hydraulics and dryout heat flux with WABE-2D code show the extent by which macro and micro inhomogeneity can enhance the bed coolability. The experimental results of MISTEE provides a basis to suggest a so-called melt drop preconditioning i.e. deformation/pre-fragmentation of a hot melt drop immediately following the pressure trigger, being instrumental to the subsequent coolant entrainment and resulting energetics of the so-triggered drop explosion. For micro-interactions in prototypical situations (with corium), three processes, namely drop surface undercooling, nucleation and growth of solid phases, and interfacial instability and breakup are evaluated with respect to their role in fine fragmentation. A new hypothesis for rationalizing the effect of corium composition (eutectic vs. non-eutectic) on its triggerability and energetics was proposed. Overall, the MSWI research in 2006-2007 has advanced a knowledge base much needed to reduce conservatism in quantification of ex-vessel melt risks in BWRs.

As we go out of 2007 and enter 2008, the MSWI project's "Production Phase" requires even a higher performance, particularly in experimental areas, to obtain required data and cope with the Project schedule. Specifically, in INCO program, we will perform transient analysis of debris bed and pool formation with/without CRGT (Control Rod Guide Tube) cooling, and special attention on IGTs (Instrumentation Guide Tube) under thermal attack from core melt and debris beds. The potential impact of this activity is high, for the uncertainty in IGT behavior has significant impact on quantification of the RPV failure and subsequent melt discharge. In EXCO program, we will be completing DEFOR and Coolability Maps, with increased attention paid to the development of experimental capability, and more importantly, to effectively sustain know-how, particularly in simulant materials selection and high-temperature melt generation. In SEE program**,** the focus is placed on mechanistic modeling, simulation and analysis of micro-interactions (complex phenomena), that enables capitalizing on the MISTEE capability and data.

References

2006-2007 Project References and Papers Published:

1. ***Proceedings of the 22nd Project Review Meeting MSWI-22 for "Melt-Structure-Water Interactions in a Severe Accident" Project***, Royal Institute of Technology, Stockholm, Sweden, May 2006, 105p.
2. ***Proceedings of the 23rd Project Review Meeting MSWI-23 for "Melt-Structure-Water Interactions in a Severe Accident" Project***, Royal Institute of Technology, Stockholm, Sweden, November 2006, 156p.
3. ***Proceedings of the 24th Project Review Meeting MSWI-24 for "Melt-Structure-Water Interactions in a Severe Accident" Project***, Royal Institute of Technology, Stockholm, Sweden, June 2007, 137p
4. C.T. Tran and T.N. Dinh, ***Analysis of Melt Pool Heat Transfer in a BWR Lower Head***, Transaction of the American Nuclear Society, Vol. 95, pp. 629-631, Nov 2006.
5. P. Kudinov, A. Karbojian, W.M. MA, M. Davydov and T.N. Dinh, ***A Study of Ex-Vessel Debris Formation in a LWR Severe Accident***, International Conference on Advances in Nuclear Power Plants, ICAPP-2007, Nice, France, May 13-18, 2007.
6. C.T. Tran, and T.N. Dinh, ***An Effective Convectivity Model for Simulation of In-Vessel Core Melt Progression in Boiling Water Reactor***, International Conference on Advances in Nuclear Power Plants, ICAPP-2007, Nice, France, May 13-18, 2007.
7. W.M. Ma and T.N. Dinh, ***Coolability Analysis of Bottom-Fed Debris Bed in a LWR Severe Accident***, 15th International Conference on Nuclear Engineering Nagoya, Japan, April 22-26, 2007, ICONE15-10472.
8. W.M. Ma, T.N. Dinh, M. Buck and M. Burger, ***Analysis of the Effect of Bed Inhomogeneity on Debris Coolability***, 15th International Conference on Nuclear Engineering Nagoya, Japan, April 22-26, 2007, ICONE15-10452.
9. A. Karbojian, W. Ma, P. Kudinov, M. Davydov and T.N. Dinh, ***A Scoping Study of Debris Formation in DEFOR Experimental Facility***, 15th International Conference on Nuclear Engineering Nagoya, Japan, April 22-26, 2007, ICONE15-10620.
10. R.C. Hansson, H.S. Park and T.N. Dinh, ***Simultaneous High Speed Digital Cinematographic and X-ray Radiographic Imaging of a Multi-Fluid Interaction with Rapid Phase Changes***, 6th International Conference on Multiphase Flow, ICMF 2007, Leipzig, Germany, July 9 – 13, 2007
11. C.T. Tran and T.N. Dinh, ***Simulation of core melt pool formation in a reactor pressure vessel lower head using an effective convectivity model***, 12th International Topical Meeting on Nuclear Reactor Thermal Hydraulics, NURETH12-072, Pittsburgh, Pennsylvania, USA, Sept.30-Oct.4, 2007.
12. P. Kudinov and T.N. Dinh, ***A analytical study of mechanisms that govern debris packaging in a LWR severe accident***, 12th International Topical Meeting on Nuclear Reactor Thermal Hydraulics, NURETH12-247, Pittsburgh, Pennsylvania, USA, Sept.30-Oct.4, 2007.
13. W.M. Ma and T.N. Dinh, ***A study on effects of debris bed prototypicality on coolability***, 12th International Topical Meeting on Nuclear Reactor Thermal Hydraulics, NURETH12-173, Pittsburgh, Pennsylvania,USA, Sept. 30-Oct. 4, 2007.
14. T.N. Dinh, ***Material property effect in steam explosion energetic: Revisited***, 12th International Topical Meeting on Nuclear Reactor Thermal Hydraulics, NURETH12-1150, Pittsburgh, Pennsylvania,USA, Sept. 30-Oct. 4, 2007.
15. R.C. Hansson, H.S. Park and T.N. Dinh, ***Dynamics and preconditioning n a single drop vapor explosion***, 12th International Topical Meeting on Nuclear Reactor Thermal Hydraulics, NURETH12-238, Pittsburgh, Pennsylvania,USA, Sept. 30-Oct. 4, 2007.

16. L. Dombrovsky, ***Large-cell model of radiation heat transfer in multiphase flows typical for fuel–coolant interaction***, International Journal of Heat and Mass Transfer, 50: 3401–3410, 2007.
17. L. Dombrovsky and T.N. Dinh***, The effect of thermal radiation on the solidification dynamics of metal oxide melt droplets***, Under review for *Nuclear Engineering and Design.*

Bibliographic Data Sheet **NKS-160**

Title	Ex-Vessel Corium Coolability and Steam Explosion Energetics in Nordic Light Water Reactors
Author(s)	T.N. Dinh, W.M. Ma, A. Karbojian, P. Kudinov C.T. Tran and C.R. Hansson
Affiliation(s)	Royal Institute of Technology (KTH), Sweden
ISBN	978-87-7893-225-9
Date	March 2008
Project	NKS-R / EXCoolSE
No. of pages	69
No. of tables	4
No. of illustrations	38
No. of references	95

Abstract

This report presents advances and insights from the KTH's study on corium pool heat transfer in the BWR lower head; debris bed formation; steam explosion energetics; thermal hydraulics and coolability in bottom-fed and heterogeneous debris beds.

This report presents advances and insights from the KTH's study on corium pool heat transfer in the BWR lower head; debris bed formation; steam explosion energetics; thermal hydraulics and coolability in bottom-fed and heterogeneous debris beds.

Specifically, for analysis of heat transfer in a BWR lower plenum an advanced three-dimensional simulation tool was developed and validated, using a so-called effective convectivity approach and Fluent code platform. An assessment of corium retention and coolability in the reactor pressure vessel (RPV) lower plenum by means of water supplied through the Control Rod Guide Tube (CRGT) cooling system was performed. Simulant material melt experiments were performed in an intermediate temperature range (1300-1600K) on DEFOR test facility to study formation of debris beds in high and low subcooled water pools characteristic of in-vessel and ex-vessel conditions. Results of the DEFOR-E scoping experiments and related analyses strongly suggest that porous beds formed in ex-vessel from a fragmented high-temperature debris is far from homogeneous. Calculation results of bed thermal hydraulics and dryout heat flux with a two-dimensional thermal-hydraulic code give the first basis to evaluate the extent by which macro and micro inhomogeneity can enhance the bed coolability. The development and validation of a model for two-phase natural circulation through a heated porous medium and its application to the coolability analysis of bottom-fed beds enables quantification of the significant effect of dryout heat flux enhancement (by a factor of 80-160%) due to bottom coolant injection. For a qualitative and quantitative understanding of steam explosion, the SHARP system and its image processing methodology were used to characterize the dynamics of a hot liquid (melt) drop fragmentation and the volatile liquid (coolant) vaporization. The experimental results provide a basis to suggest that the melt drop preconditioning is instrumental to the subsequent coolant entrainment and resulting energetics of the so-triggered drop explosion. For steam explosion risk in reactors, a revisited study of the material property effect on steam explosion energetics showed that corium high density, high melting point and low conductivity are central to mechanisms in premixing that govern corium low explosivity.

Key words Severe Accident, Corium, Debris Bed, Coolability, Steam Explosion

Available on request from the NKS Secretariat, P.O.Box 49, DK-4000 Roskilde, Denmark.
Phone (+45) 4677 4045, fax (+45) 4677 4046, e-mail nks@nks.org, www.nks.org